HOKKAIDO UNIVERSITY

Title	Internal Friction of Ice. I ; The Internal Friction of H2O and D2O Ice, and the Influence of Chemical Impurities on Mechanical Damping
Author(s)	KUROIWA, Daisuke
Citation	Contributions from the Institute of Low Temperature Science, A18, 1-37
Issue Date	1964-03-25
Doc URL	https://hdl.handle.net/2115/20227
Type	departmental bulletin paper
File Information	A18_p1-37.pdf

Hokkaido University Collection of Scholarly and Academic Papers : HUSCAP

Internal Friction of Ice. I

The Internal Friction of H_2O and D_2O Ice, and the Influence of Chemical Impurities on Mechanical Damping*

By

Daisuke KUROIWA

黒岩大助

Physics Section, The Institute of Low Temperature Science.

Received January 1964

Abstract

The internal friction of pure H_2O, D_2O ice and contaminated ice crystals containing various chemical impurities such as NaCl, HCl, NaOH, HF and NH_4F were measured, between 0°C and −180°C, by the flexural vibration method. The following results were obtained: (1) in pure H_2O and D_2O ice, a typical relaxation curve was observed showing the same value for the activation energy (13.1 kcal/mole) as for the dielectric relaxation, (2) in doped ice crystals, the activation energy was reduced to about half of the pure ice value, (3) another damping maximum due to aggregated impurities appeared around −145°C in NaCl- and HCl-doped ice, (4) this maximum decreased with annealing, (5) fluoride-doped ice crystals also exhibited an annealing effect on the relaxation curve.

Contents

I. Introduction 2
II. Experimental Methods 3
III. The Temperature Dependence of Internal Friction of Pure H_2O and D_2O Ice Crystals 5
IV. The Influence of Various Chemical Impurities on Mechanical Damping 12
1. Modification of Mechanical Damping due to the NaCl, HCl, and NaOH

* Contribution No. 667 from the Institute of Low Temperature Science.

2. Impurity Distribution in NaCl, HCl and NaOH doped Ice Crystals
3. Modification of Mechanical Damping as a Function of NaCl Concentration
4. Modification of Mechanical Damping due to HF and NH_4F
V. Resultant Mechnical Damping Curves of Artificially Combined Ice Crystals 32
VI. Anisotropy of the Height of Maximum Damping due to Crystallographic Orientation, and the Influence of Plastic Deformation on Maximum Damping 34
VII. Concluding Remarks 36
References 37

I. Introduction

When a solid bar is set into free vibration, the amplitude of its oscillations decreases with time. This is true even if the bar is completely isolated from its surrounding so that radiated sound losses and similar effects are negligible. This dissipation of vibrational energy is caused by internal friction. The internal friction (mechanical damping) of the solid bar is so structure sensitive that it has been used as one of the more fundamental methods of analyzing the internal structure of a crystalline solid in that damping can arise from crystal imperfections, such as lattice defects, chemical impurities, and inclusions.

When the measured internal friction (denoted as $\tan\delta$) of a crystalline solid can be expressed by the following relationship:

$$\tan\delta = (\tan\delta)_{\max}\frac{2\omega\tau}{1+\omega^2\tau^2} \qquad (1)$$

and

$$\tau = \tau_0 \exp\left(\frac{Q}{RT}\right), \qquad (2)$$

where ω is an angular frequency, τ is the relaxation time, Q is the activation energy, R is the gas constant, T is the absolute temperature, and τ_0 is constant, one can attribute one of the possible mechanisms of mechanical damping to simple atomic movement (diffusion) through the lattice defects.

Several measurements of the internal friction of ice have been made by various authors using different techniques. KNESER *et al.* (1955) observed mechanical damping of a single ice crystal at temperatures ranging from 0°C to −25°C by means of torsional vibrations. They found that a single crystal of ice exhibits a typical mechanical relaxation phenomenon which can be expressed by the given equations. They obtained 8.5 kcal/mole as a value for

the activation energy. KUROIWA and YAMAJI (1956, 1959) measured, by the flexural vibration method, the internal friction of both polycrystalline and single-crystal ice in wide temperature ranges between 0°C and −180°C. They found that there are three kinds of mechanical damping produced by grain boundaries, proton movement, and chemical impurities. The observed activation energy due to the proton movement was about 6 kcal/mole. Recently, SCHILLER (1958) observed the mechanical relaxation of a pure single ice crystal by means of longitudinal and torsional vibrations. He found that the mechanical damping of a single ice crystal changed with crystallographic orientation and the mode of oscillation used. The observed activation energy was 13.4 kcal/mole.

Ice crystals exhibit a remarkable mechanical relaxation phenomenon like that of "anelasticity" in metals. Although it is believed that mechanical relaxation in ice crystals is caused by proton movement through lattice defects, some discrepancies are found among the experimental data. The author believes that these discrepancies may be mainly attributed to the chemical impurities involved. The present study was undertaken in order to reveal how the chemical impurities exert their influence on the mechanical damping of ice. At the onset, pure H_2O and D_2O ice were studied to determine the temperature dependence of internal friction. Some differences in relaxation times due to the heavier mass of deutron was observed in D_2O ice. The main part of this paper is devoted to the investigation of doped ice crystals containing known chemical impurities such as NaCl, HCl, NaOH, HF, NH_3, and NH_4F. The effect of mechanical damping due to grain boundaries was clarified by a special technique which permitted measurement of the internal friction between the individual grain-boundaries of polycrystalline ice. The internal friction at grain boundaries is not always proportional to the total area of the boundary, but is influenced by the chemical impurities concentrated in the boundary zone. These experimental data also provided an explanation for the characteristic mechanical damping curves obtained for natural glacier ice.

II. Experimental Methods

Internal friction is expressed as a logarithmic decrement in free oscillation. In our experiment, a flexural vibration was used for measurement of internal friction as shown in Fig. 1. The vibration apparatus was placed in a cold box which could be refrigerated with liquid oxygen or nitrogen. P_1 and P_2 are rectangular ice bars cut from the same ice block and trimmed to exactly the same dimensions. Both ice specimens were cooled at the same rate. P_1 was used for temperature determination, and P_2 for mechanical damping. Thin iron bands I_1 and I_2 were attached to the ends of P_2. An exciting coil C_1 and

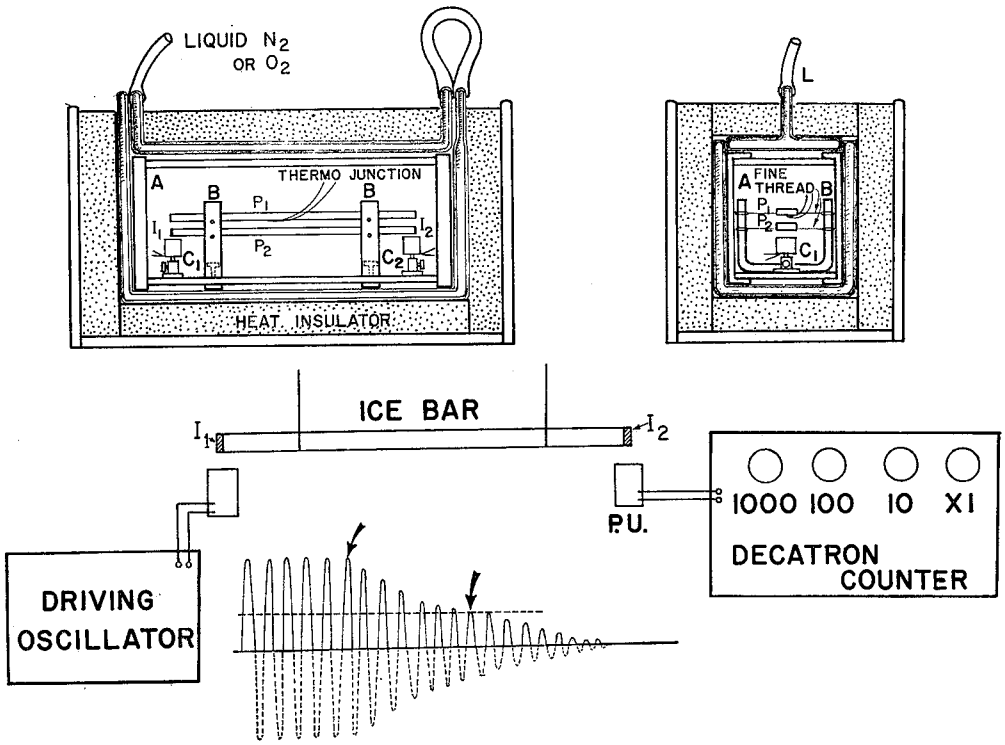

Fig. 1. Scheme of the experimental apparatus

a pick-up coil C_2 were placed about 5 mm below iron bands I_1 and I_2, respectively. P_1 and P_2 were suspended at their vibration nodal points with two fine silk threads stretched between the metal U-shaped brackets B. Alternating current was supplied to the coil through an audio frequency oscillator. When the A. C. frequency matched the proper vibrational frequency of P_2, resonance took place, and the induced current in the pick-up coil C_2 then reached a maximum value. At this moment, if the current in C_1 is short circuited, the specimen P_2 begins a damped free oscillation. According to the theory of oscillation, the logarithmic decrement Δ is given by;

$$\Delta = \frac{\ln n}{f \times t(1/n)} \qquad (3)$$

where, f is a resonant frequency, $t(1/n)$ the time required for the amplitude to decrease to $1/n$ of its original value, and n is an integer.

In order to measure Δ, a special electronic device was used. The induced voltage in the pick-up coil C_2 was introduced to a "pulse counter" which

consisted of 4 electronic pulse-counter tubes (commercial name; Decatron). The Decatron tube records every peak oscillation. If we previously set a working voltage on the counter, so that the Decatron tubes will operate from the beginning of free oscillation until the amplitude drops to $1/n$ of the initial value, (operating period is between the two arrows indicated in Fig. 1) the total number of oscillations N indicated on the 4-stage Decatron is equal to $f \times t(1/n)$. One can easily obtain the internal friction $\tan\delta$ by

$$\tan\delta = \frac{\Delta}{\pi} = \frac{\ln n}{\pi N} = \frac{\text{constant}}{N} . \qquad (4)$$

The resonant frequency of P_2 can also be measured by this apparatus.

The internal friction of all ice specimens was measured as a function of both temperature and frequency. The apparatus upon which the ice specimen was mounted was enclosed in a refrigerated cold box. Measurement of the temperature of the specimen P_2 was found by measuring the temperature of P_1 which had the same dimensions as P_2. The temperature of the specimen reached that of liquid nitrogen about 2 hours after the refrigerant was supplied into the cold box. The damping measurments were taken after stopping the coolant flow, and as the insulated box was slowly warming up.

The resonant frequency of a rectangular bar is given by

$$f = \left\{ \frac{m^4 a^2 E}{48\pi l^4 \rho} \right\}^{1/2} \qquad (5)$$

where, E is an elastic modulus, l is the length of the specimen, a is its thickness, ρ is the density, and m is a constant determined by the mode of oscillation. As shown in equ. (5), the frequency of the specimen is a function of a, l, and m. The following numerical values of the constant m were used; 4.75 for the fundamental vibration, and 7.85 for the 1st overtone. It was difficult to change the resonant frequency for the wide ranges because of the limited size of the specimen.

III. The Temperature Dependence of Internal Friction of Pure H_2O and D_2O Ice Crystals

Pure H_2O ice was made by freezing distilled water, filtered through an ion-exchange resin, in a polyethylene container. A rectangular ice bar was cut from the transparent part of the frozen ice block. A microtome was used to trim the ice bar precisely 196 mm long, 11.8 mm wide, and 3.7 mm thick. In order to eliminate just the mechanical strain which could be created by the trimming, the specimen was put in a plastic envelope and kept at $-10°C$ for

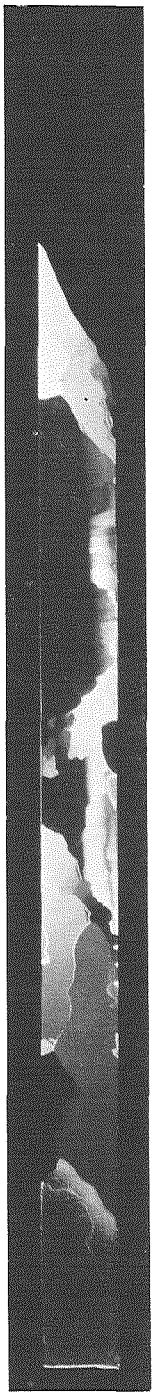

Fig. 2. Grain structure of pure ice specimen taken under polarized light

one or two days. A photograph of this specimen taken under polarized light is shown in Fig. 2. The specimen consists of many large randomly oriented grains.

In Fig. 3, curves (1) and (2) represent the typical temperature dependence of internal friction in pure ice measured at the fundamental and the first overtone frequencies, respectively. These curves exhibit a remarkable sharp maximum damping. The resonant frequencies at the maximum damping of these curves were 297 c.p.s. for the fundamental and 816 c.p.s for the first overtone. The temperatures at which the maximum damping occurred were found to be -31.5°C for the fundamental and -22°C for the first overtone. Curve (3), the fundamental, and curve (4), the first overtone, show the mechanical relaxations for the same specimen after the thickness and width were reduced to 2.4 mm and 11 mm, respectively. As shown in Fig. 3, the locations of the damping maxima shifted toward higher temperature ranges as frequency increased with a slight decrease in $\tan\delta$. In these experiments, the height of maximum damping of the pure H_2O ice occurred approximately between 0.0085 and 0.0095. The sharpness of the relaxation curves may be expressed as width ΔT, where $\tan\delta$ is half the maximum. The mean value of ΔT was found to be about 25°C. The slope of the relaxation curves tended to extremely low values and no peculiarity was observed as the temperature was lowered to -190°C. A steep rise of $\tan\delta$ was found as the temperature approached the melting point. The deviation from the relaxation curve in the high temperature range is due to grain boundary internal friction.

In the right hand corner of Fig. 3, the observed mechanical damping of another specimen of pure ice is illustrated as the function of temperature and frequency. Resonant frequency at maximum damping is indicated on each curve.

Electrical resistivity of a melted specimen, measured at room temperature, was used to determine the chemical impurity index. The electrical resistivity of the melted pure ice specimen was about 1300 kohm cm. The electrical resistivity of doped ice can be expected to be much lower.

Liquid D_2O obtained from Volk Co., Chicago Ill., USA

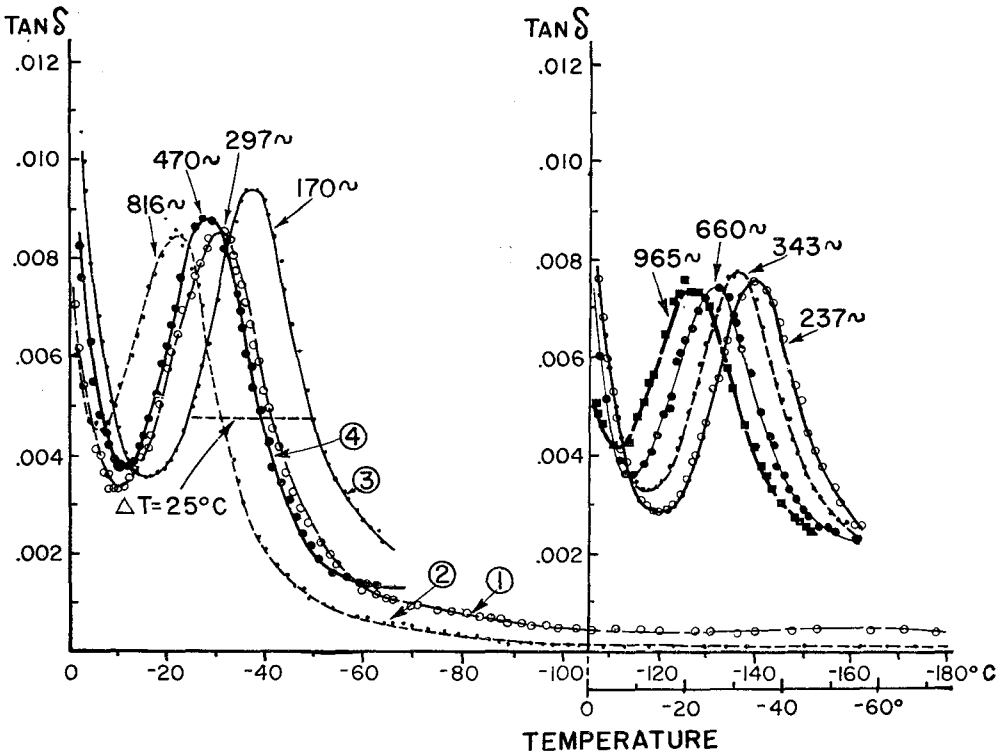

Fig. 3. Temperature dependence of internal friction in pure polycrystalline ice

was frozen into a rectangular bar and prepared in the same manner as the H_2O block. The average grain size was similar to that of Fig. 2. Figure 4, illustrates the typical temperature dependence of mechanical damping for D_2O ice. Damping maxima were observed between $-10°C$ and $-40°C$, showing that their locations shift towards the higher temperature ranges with increased vibrational frequency. The resonant frequencies at the damping maxima are indicated on each curve. The measured temperatures for several of the curves were extended to $-190°C$, but the slopes of the relaxation curves tended to the lower values and no peculiarity was found. In the high temperature range, however, the steep rise of $\tan\delta$ caused by the crystal boundaries appeared as the temperature approached the melting point. The average value for maximum damping and the sharpness of the relaxation curves are identical to those obtained for pure H_2O ice.

Figure 5, represents the relation between logarithmic plots of the relaxation time τ and the reciprocal of absolute temperature T^{-1}, at which the damping maxima appear. The relaxation time is given by the reciprocal of the angular

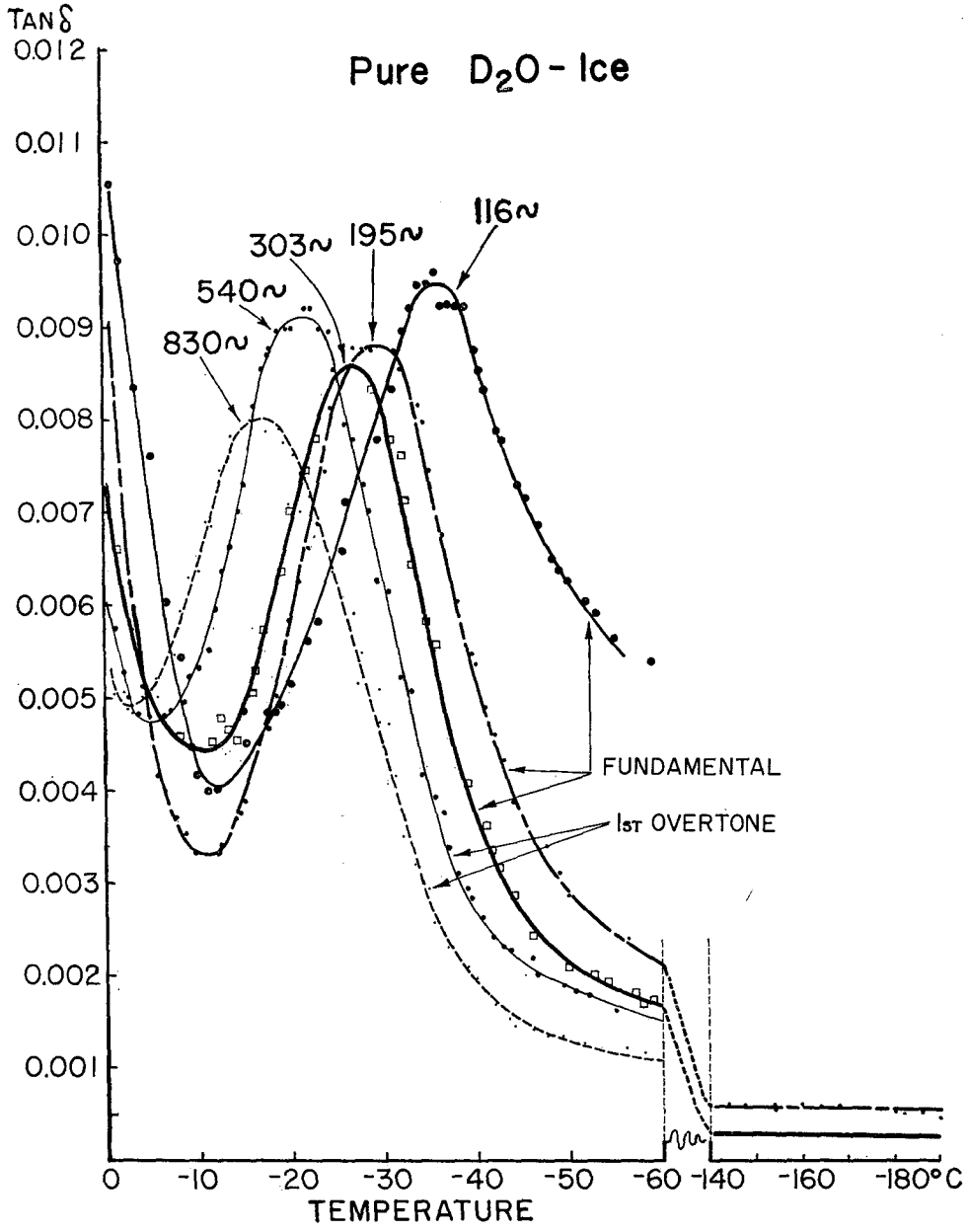

Fig. 4. Temperature dependence of internal friction in pure D_2O-ice

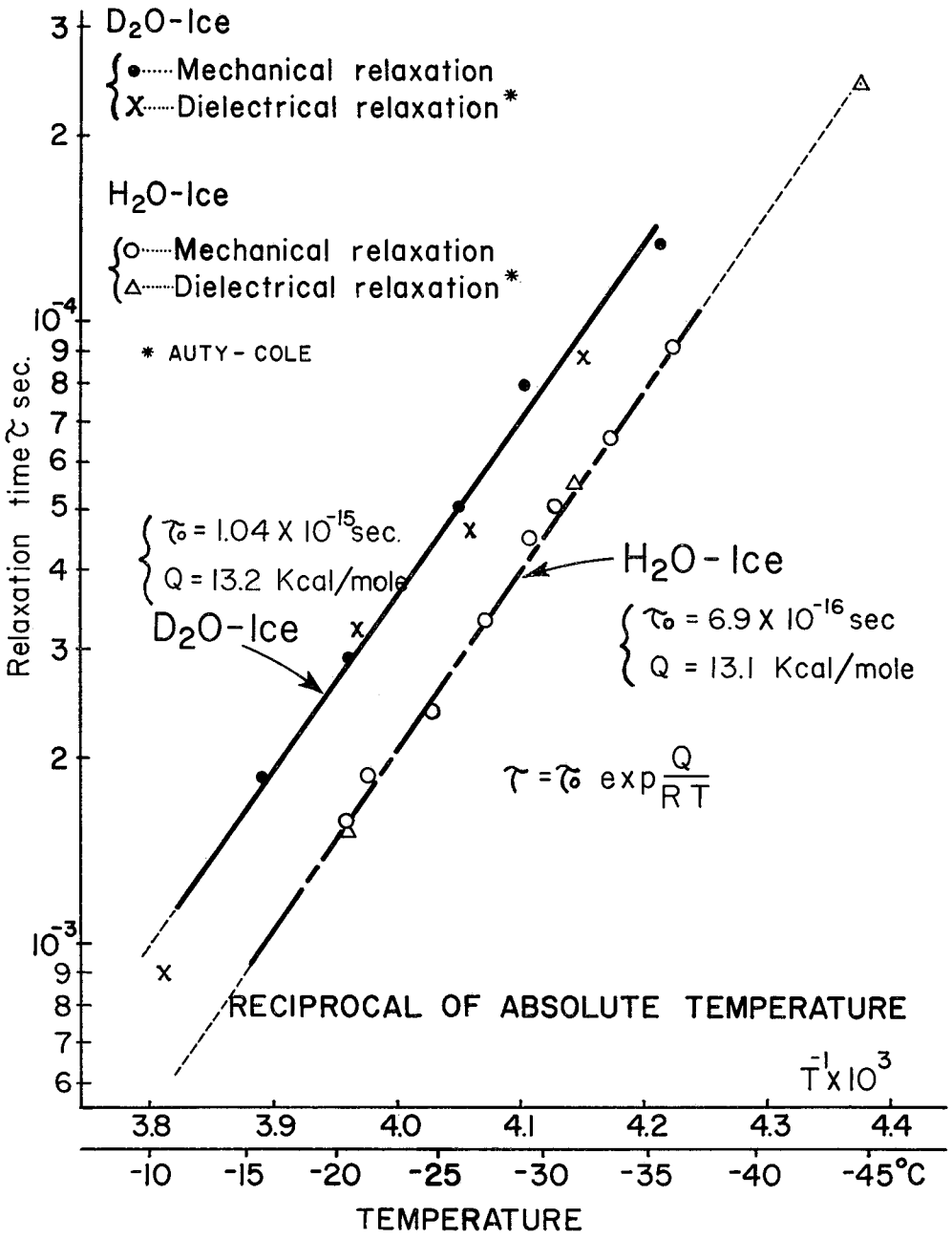

Fig. 5. Relation between relaxation time of pure H_2O- and D_2O-ice and the reciprocal of absolute temperature

frequency at which maximum damping occurs. The relationships for pure H_2O (white circle) and for D_2O (black circle) ice are expressed well by ARRHENIUS's equation (2). The dielectric relaxation times measured by AUTY-COLE (1952) in the same temperature range also are plotted with two symbols (△ for the pure H_2O ice, and × for the D_2O ice). They are also distributed well along each straight line, implying that both the mechanical and the dielectrical relaxation process are originated by the same mechanism of proton movement. This observation is felt to be the most important outcome of the present work. GRÄNICHER *et al.* (1957), have explained the dielectric relaxation in pure ice in terms of dipole rotation through D- and L-defects, as suggested by BJERRUM (1952). In a perfect ice crystal, only one hydrogen atom lies on the line connecting two neighboring oxygen atoms. In nonperfect ice crystals, however, the following two imperfections can exist in the lattice; the O–O linkage is occupied by two hydrogen atoms (D-defect), or no hydrogen atoms lie on the O–O linkage (L-defect). By rotation of a molecule adjacent to a D- or L-defect, the defect moves to a neighboring linkage and is thus able to diffuse in the crystal. The diffusion of these crystal imperfections cause reorientation of the proton and can lead to energy dissipation under the applied electrical field.

The observed constant τ_0 and activation energy Q were found to be;

$\tau_0 = 6.9 \times 10^{-16}$ sec. $\quad Q = 13.1$ kcal/mole, for pure H_2O ice.
$\tau_0 = 1.04 \times 10^{-15}$ sec. $\quad Q = 13.2$ kcal/mole, for D_2O ice.

The evaluation of these numerical values always involves some error since they were obtained from the slope of the curve on a logarithmic scale. In our experiment, the resulting error can be considered to be about 5 percent. As shown in Fig. 5, the observed relaxation time of D_2O ice is longer than that of the pure H_2O ice. The ratio of preexponential factors $\tau_0(D_2O)/\tau_0(H_2O)$ is 1.5. This may be explained by the difference in mass between deutron and proton.

The good agreement of the observed damping curve with the theoretical curve is shown in Fig. 6 (bottom). The solid curve represents the observed data and the dotted curve that calculated from equs. (1) and (2), using the following numerical values; $\tau_0 = 6.9 \times 10^{-16}$ sec, $Q = 13.1$ kcal/mole, $\tan \delta_{max} = 0.0085$, $f = 297$ c.p.s. Deviations from the calculated curve are shown by the shaded area. The shaded area in the high temperature range is due to grain-boundary internal friction, and in the low temperature range it is caused by radiated sound loss, and loss of energy through the suspending threads. The agreement of the curves indicates that the mechanical damping of ice is caused by a single relaxation mechanism. The deviation of the resonant frequency

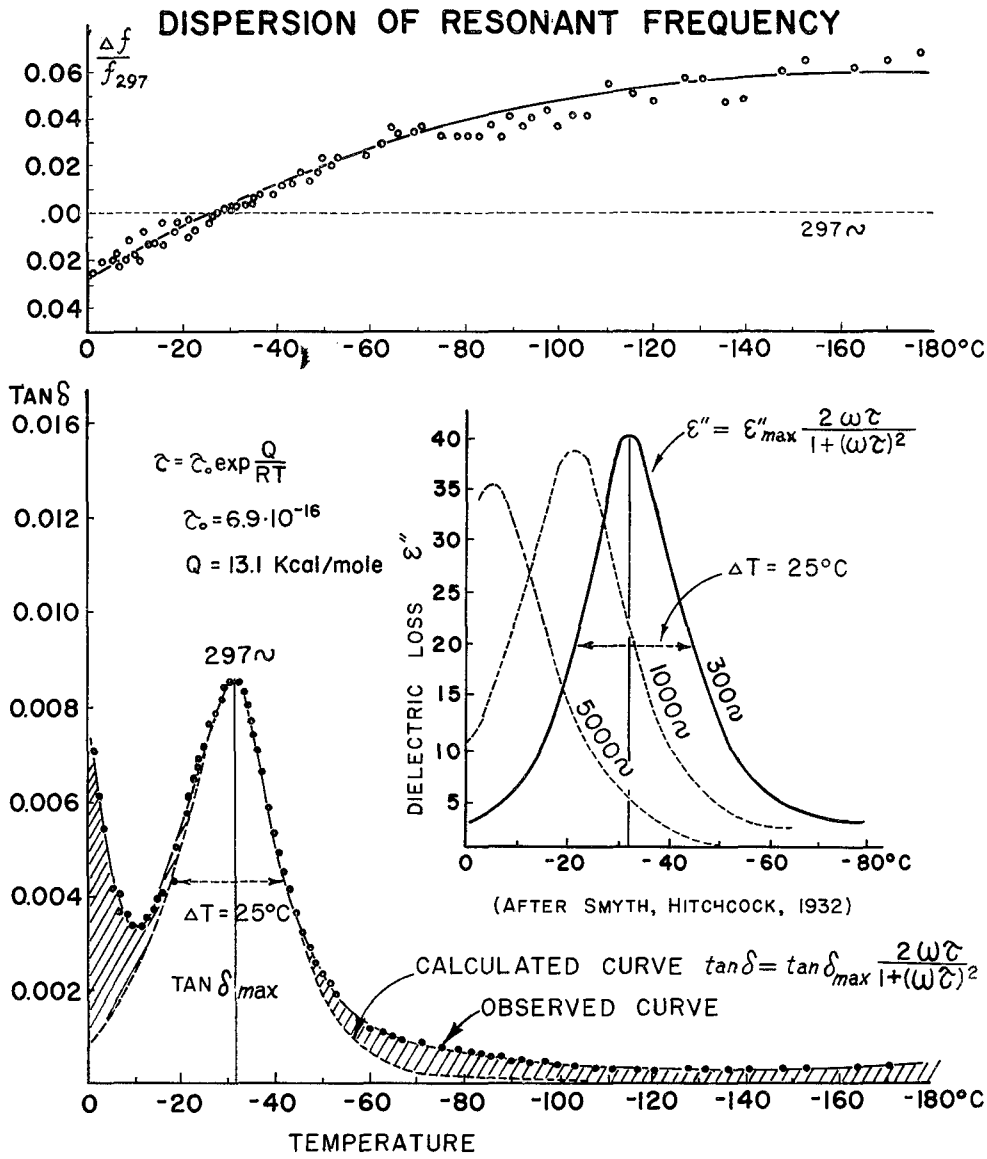

Fig. 6. Comparison between the observed curve and the calculated curve for pure H_2O ice having a single relaxation time, and the dielectric loss curves obtained by SMYTH and HITCHCOCK

from that of maximum damping is plotted versus temperature in the upper part on Fig. 6. Resonant frequency dispersion and maximum damping took place in the same temperature range.

The dielectric loss ε'' of a pure ice crystal measured by SMYTH and HITCHCOCK (1932) is depicted as a function of temperature in the middle part of Fig. 6. The temperature dependence of ε'' of the pure ice is also expressed by equs. similar to (1) and (2). As shown in this figure, the maximum of dielectric loss shifted towards the high temperature range with an increase in frequency, and showed a slight decrease in the curve height. Comparison of both the mechanical damping curve and the dielectric loss curve measured at 300 c.p.s. shows a similar temperature dependence and sharpness ($\Delta T = 25°C$).

IV. The Influence of Various Chemical Impurities on Mechanical Damping

Mechanical and dielectrical relaxation phenomena in ice crystals can be explained by proton movement through lattice defects. When doped ice is crystallized in water containing chemical impurities, some chemical additives may be captured. Since the lattice configuration near the captured impurities would be strongly modified, many lattice imperfections may be formed. The influence of chemical impurities on dielectric relaxation of ice has been studied by various authors, but a systematic investigation for mechanical relaxation has not yet been conducted. In this section, the results of the experimental investigation are discussed. In the experiment, NaCl, HCl, and NaOH were used as neutral, acidic, and alkalic additives which may behave as interstitial lattice modifiers. HF and NH_4F were used as a substitutional lattice modifiers in the ice crystal.

1. *Modification of Mechanical Damping due to NaCl, HCl, and NaOH*

With the aid of NaCl, a typical neutral compound, a modification of mechanical damping was shown from the onset. A dilute aqueous solution containing 0.001 mole of NaCl was frozen in the cold room. A rectangular bar was cut from the doped ice block, and prepared in the same manner as before. The specimen consisted of large randomly oriented grains. The actual concentration of NaCl in the ice crystal was not measured, but the electrical resistivity for the melted specimen was 350 kohm cm, which is lower than the value for pure ice, indicating the existence of NaCl.

Figure 7 depicts the effect of temperature variation on mechanical damping of NaCl ice. Several modifications were observed. The width, ΔT, of the relaxation curves due to proton diffusion, became broader than that of pure

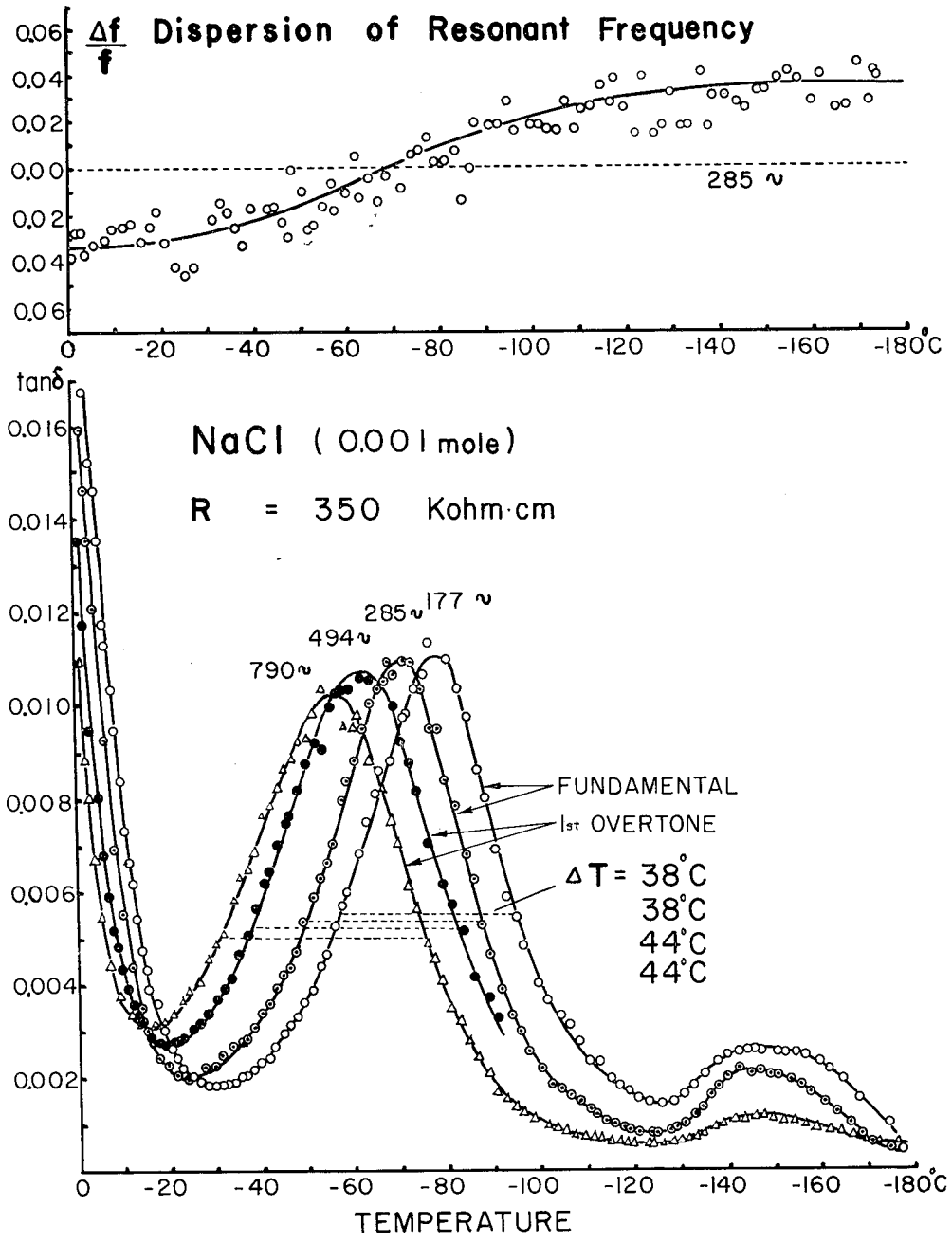

Fig. 7. Temperature dependence of internal friction in NaCl doped ice crystal

H_2O ice, average $\Delta T = 41°C$ at $\frac{1}{2}(\tan\delta)_{max}$. The location of these damping maxima appeared in a lower temperature range than those of pure ice.

A new modification is the appearance of another damping maximum at around $-145°C$. This low temperature damping was not observed in pure H_2O and D_2O ice. As shown in Fig. 7, this maximum decreased inversely to the vibrational frequency, but an appreciable shift of its location was not observed. A steeper rise in grain boundary internal friction appeared near

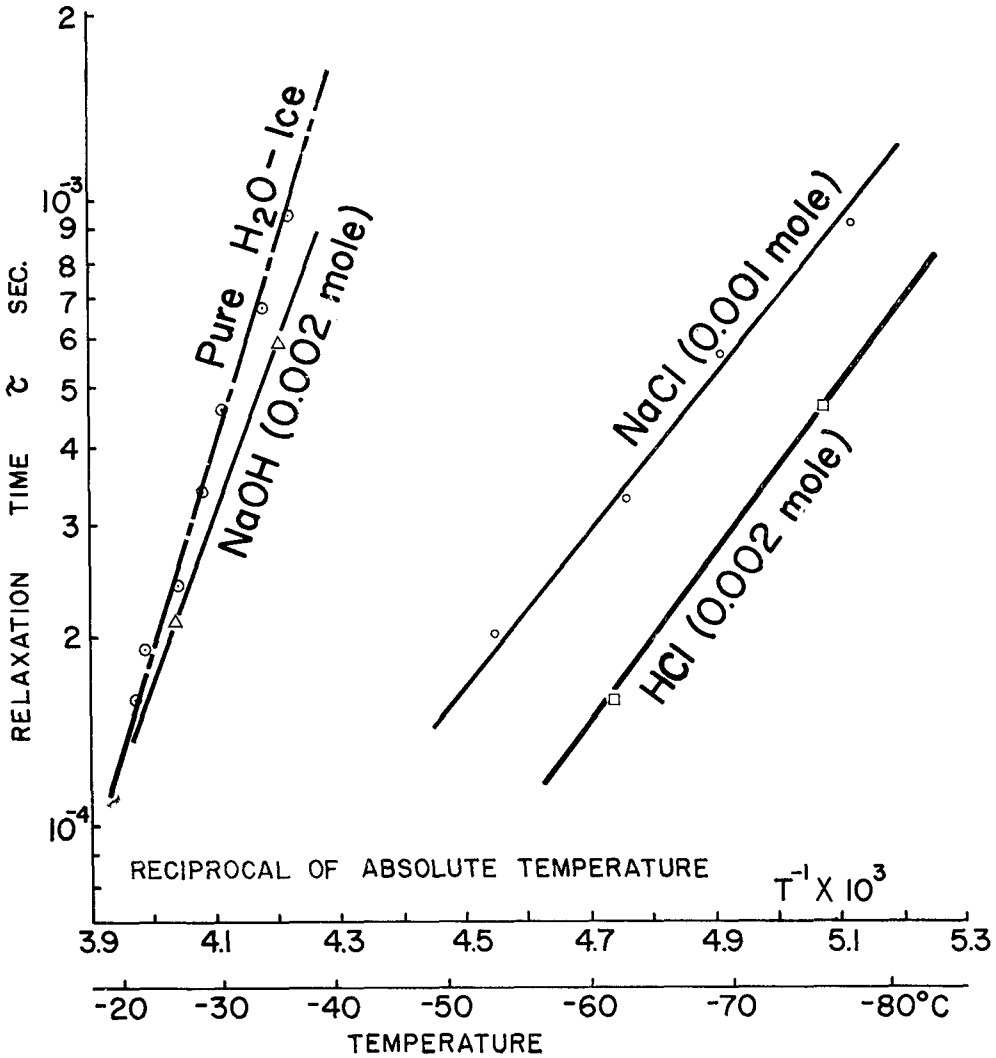

Fig. 8. Relaxation time of various doped ice crystals and the reciprocal of absolute temperature

the melting point.

The dispersion of resonant frequency is shown in the upper part of Fig. 7. The deviation of resonant frequency from f_{max}(285 c.p.s.) at which maximum damping occurs was plotted as a function of temperature. As shown by a soild curve, a steep variation of the resonant frequency occurs at the some intermediate temperature as maximum damping (lower figure) due to proton movement. No appreciable dispersion was observed in either high or low temperature ranges where $\tan\delta$ rose steeply and another damping maximum appeared. The relation between relaxation time and reciprocal of absolute temperature, both obtained from the resonant frequency and temperature at maximum damping, is plotted in Fig. 8. From the slope of this curve, Q and τ_0 are found to be 5.57 kcal/mole and 3.95×10^{-10} sec., respectively. These constants differ greatly from those of pure H_2O ice.

An acidic doped ice crystal was made by freezing a dilute acid solution containing 0.002 mole of HCl. A rectangular ice bar (190 mm long, 17.1 mm wide, 4 mm thick) was prepared from this ice block. The electrical resistivity of the melted specimen was 300 kohm cm. Figure 9 represents the temperature dependence of the mechanical damping of HCl-ice measured at the fundamental, and at the first overtone vibrations. Modification of mechanical damping due to HCl was the same as that caused by NaCl. The relaxation curve due to proton movement became broad (mean $\Delta T=40$°C). The steep rise of $\tan\delta$ and mound-like damping appeared at high and low temperature ranges, but no temperature shift was observed in the mound-like damping. The relation between logarithmic plots of the relaxation time and the reciprocal of absolute temperature for maximum damping (see Fig. 8) gave the following numerical values: $Q=$ 6.0 kcal/mole, $\tau_0=8.95\times10^{-10}$ sec.

More complicated modifications of mechanical damping were observed in an alkaline doped ice crystal as depicted in Fig. 10. This specimen was prepared from an NaOH solution, concentration 0.002 mole, with an electrical resistivity of 900 kohm cm when melted. The sharp relaxation curves, $\Delta T=$ 25°C, appeared in the same temperature range as for pure H_2O ice. A peculiar damping curve was observed in the low temperature ranges, but its height decreased remarkably with frequency. The $\log\tau$ vs. T^{-1} for NaOH ice is illustrated in Fig. 8. A straight line for this specimen is located at nearly the same temperature range as pure ice, showing that $Q=11.6$ kcal/mole, $\tau_0=1.2\times10^{-14}$ sec.

2. *Impurity Distribution in NaCl, HCl and NaOH doped ice crystals.*

Experimentation revealed that mechanical damping of ice can be modified

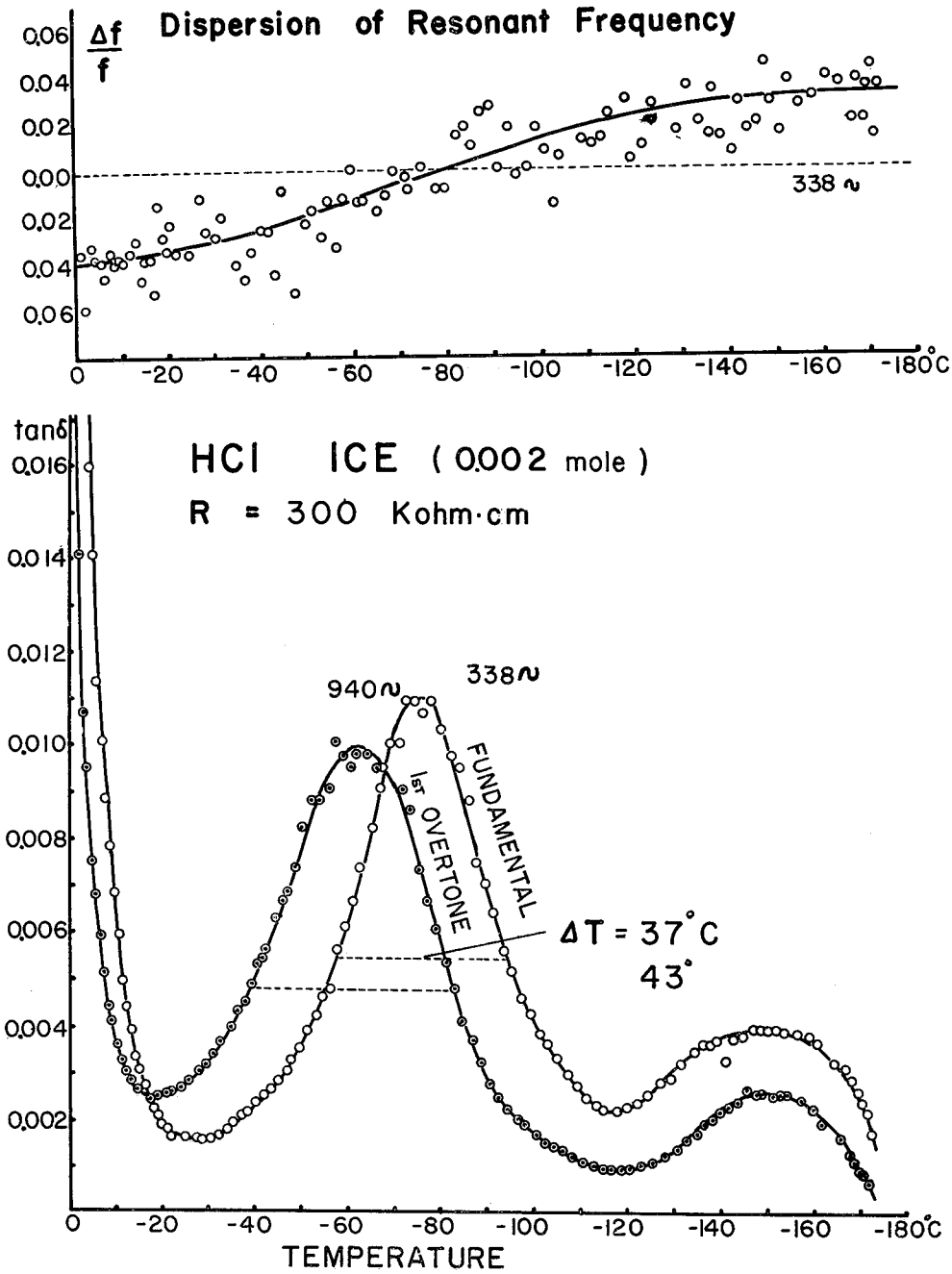

Fig. 9. Temperature dependence of tan δ in HCl-doped ice crystals

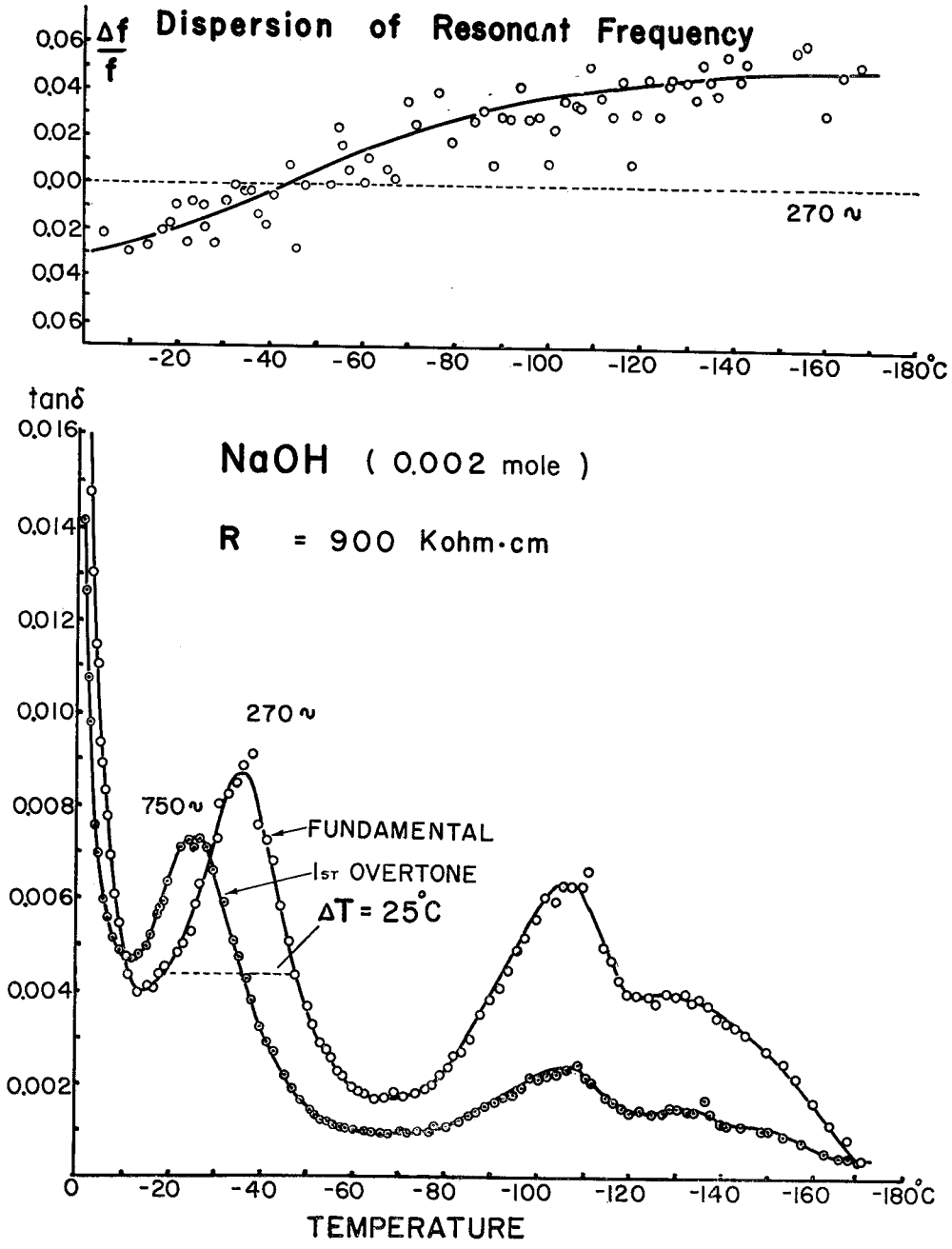

Fig. 10. Temperature dependence of tan δ in NaOH-doped ice crystals

by NaCl, HCl and NaOH. If we assume that vibrational energy is dissipated only at the site of crystal imperfections and that a close correlation exists between impurity additives and defects, the following inference can be drawn.

When a crystal grows from a melt or a solution, it is believed that most of the impurities concentrate at the crystal boundaries, but some of them can exist in an atomic or aggregated state within the grains. Each of these three types of impurity distribution may have a distinctively different influence on the mechanical damping of a crystal. In both NaCl and HCl-doped ice crystals, the relaxation curve due to proton movement became broad and the lowering of the activation energy and the shortening of the relaxation time occurred as shown in Figs. 7 to 9. The dispersion of resonant frequency can also be closely correlated with maximum damping. According to GRÄNICHER *et al.*, the energy required for the formation of a lattice defect is greater than that required for diffusion. The lowering of the activation energy and the shortening of the relaxation time, therefore, may be caused by excess lattice defects created by the impurity additives. This suggests that NaCl or HCl can disperse homogeneously within the grains in an atomic or a molecular state similar to a solid solution, and consequently may form more imperfections than can be found in pure ice, thus strongly influencing mechanical damping. TRUBY's (1952) experiment concerning the electrical properties of ice suggests that halogen ions incorporate substitutionally in the ice crystal lattice. It was difficult in our experiment, however, to determine whether NaCl and HCl exist substitutionally or interstitially in the lattice.

The mound-like mechanical damping curve which appeared around $-145°C$ suggestes that NaCl and HCl molecules can separate in aggregates at localized imperfections such as microscopic holes or pockets or vacant places. This moundlike damping has never been observed in pure ice. The temperature range of this damping did not shift, though its maximum value decreased with increasing frequency. Moreover, no dispersion in the resonant frequency occurred in the same temperature range as that of the mound-like damping. These observations indicate that the distribution and density of these imperfections may be localized in the ice crystal, and NaCl or HCl molecules may oscillate independently within such imperfections. Although a definite model for the microscopic holes or vacant places in an ice crystal lattice has not been proposed, experiments concerning the sintering of ice, by KINGERY (1960) and KUROIWA (1961), suggest the existence of this type of imperfection. The third type of distribution is a concentration at the grain boundaries. At the front of a crystal growing in solution, an accumulation of impurities takes place. When two crystals grown from different nuclei meet together, a large

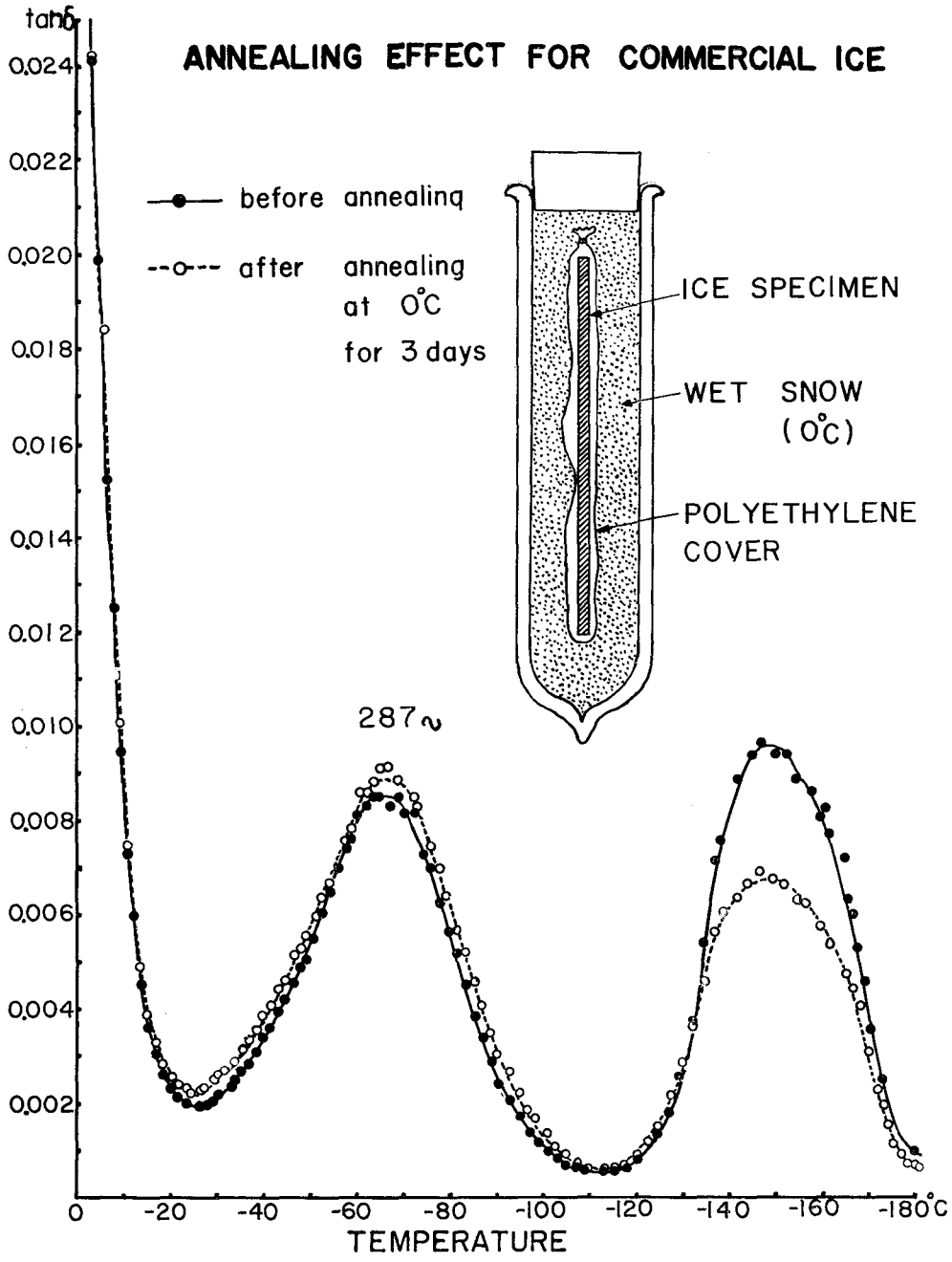

Fig. 11. Annealing effect on tan δ in commercial ice

amount of impurities can be concentrated at the crystal boundary. Grain boundary internal friction is caused by grain boundary viscosity. A detailed discussion will be given in a subsequent paper.

The most peculiar damping curve was observed in NaOH doped ice. A sharp relaxation curve, $\Delta T = 25°C$, appeared indicating that mechanical damping due to proton movement was not modified by the addition of NaOH. In fact a logarithmic plot of the relaxation time of this specimen is located in the same temperature range as pure ice (Fig. 8). The steep dispersion of resonant frequency was found only in the same temperature range as this maximum damping. The characteristic damping in the low temperature range, therefore, suggests that most NaOH molecules could be captured locally in an aggregated state.

The concentration of chemical impurities at localized crystal imperfections may depend on: crystallization velocity, affinity for the H_2O molecule, and possibly other unknown variables. Their concentration, however, might be unstable in the ice crystal lattice.

The height of the mound-like damping around $-145°C$ can be reduced by annealing (Fig. 11). In Figure 11, black circles represent internal friction of a specimen prepared from ordinary commercial ice. The actual concentration of chemical impurities involved was not known, but the electrical resistivity was 450 kohm cm. The specimen shows a remarkable damping in the low temperature range. After the first measurement, the specimen was put in a polyethylene envelope and kept in a vacuum flask filled with wet snow (0°C) for 3 days. White circles show the change in the damping curve after 3 days of annealing. Noticeable decrease in the height was observed in the low temperature damping, but no appreciable change was found in either the grain boundary or proton diffusion damping.

The distribution of localized imperfections and defects along crystal boundaries can be changed by irradiation with heat rays. A polycrystalline ice specimen was exposed to a strong infrared lamp for a few minutes, causing conspicuous internal melting at crystal boundaries and inside the grains as shown in Fig. 12. After irradiation, mechanical damping of this specimen was measured and compared with the result obtained before the treatment was applied. The low temperature mound-like damping greatly decreased and grain boundary internal friction increased remarkably, but no appreciable change was observed in the height of maximum damping due to proton movement. In Fig. 12, white and black circles indicate $\tan\delta$ before and after irradiation. The process of internal melting due to irradiation is not completely understood. NAKAYA (1956) suggested that Tyndall figures may be formed by colloidal

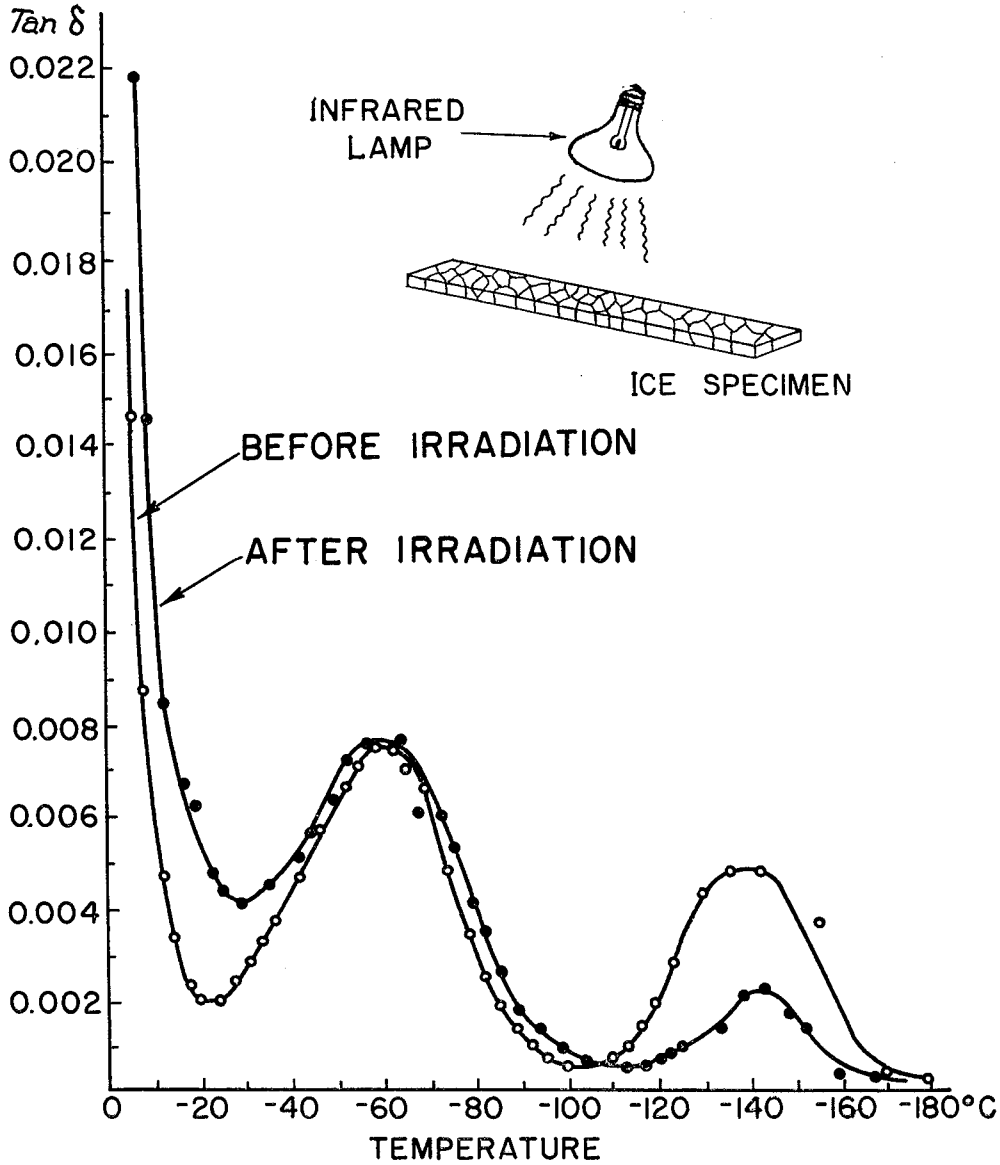

Fig. 12. Variation of internal friction due to irradiation with heat ray

particles or lattice defects absorbing the heat rays and consequently causing internal melting. It is quite natural to suppose that concentrated chemical impurities at localized imperfections would begin to melt when the temperature approaches the melting point, causing a change in the impurity distribution.

During irradiation, some chemical impurities within the grains could diffuse to the grain boundaries, greatly influencing mechanical damping. Glacier ice usually contains chemical impurities, but it does not show any mound-like damping in the low temperature range. This also can be explained by the annealing effect which glacier ice is subjected to for long periods of time—a detailed discussion of this will follow in a subsequent paper.

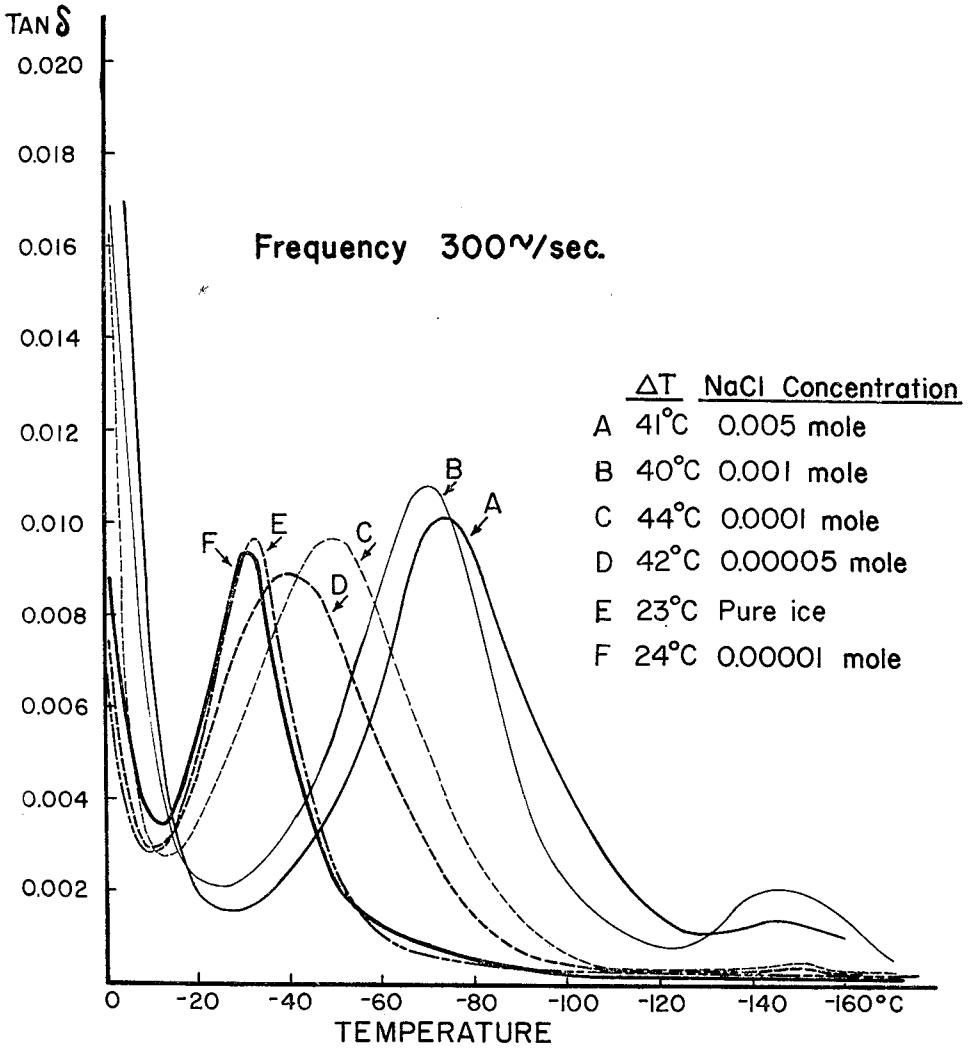

Fig. 13. Shift of the relaxation curve toward the low temperature side as a function of NaCl-concentration

3. *Modification of Mechanical Damping as a Function of NaCl Concentration*

In order to examine how the mechanical damping changes with concentration of NaCl, various ice specimens were made from aqueous solutions having different NaCl concentration. The maximum and mimimum concentrations of the mother solution were 0.005 mole and 0.00001 mole, respectively. The same volume of solution was frozen under the same cooling conditions. All specimens were trimmed to the same dimentions by means of a microtome so that they could be measured at the same frequency.

Figure 13 illustrates a typical variation of the mechanical damping as a parameter of NaCl concentration. The resonant frequency of each specimen was the same within several percent. The relaxation curve of the specimen crystallized from the most dilute solution (0.00001 mole) was approximately the same as the curve for pure ice. Good superposition of the curves is seen in the same temperature range. The relaxation curve became broad ($\Delta T = 42°C$) at concentrations above 0.00005 mole, and the location of maximum damping

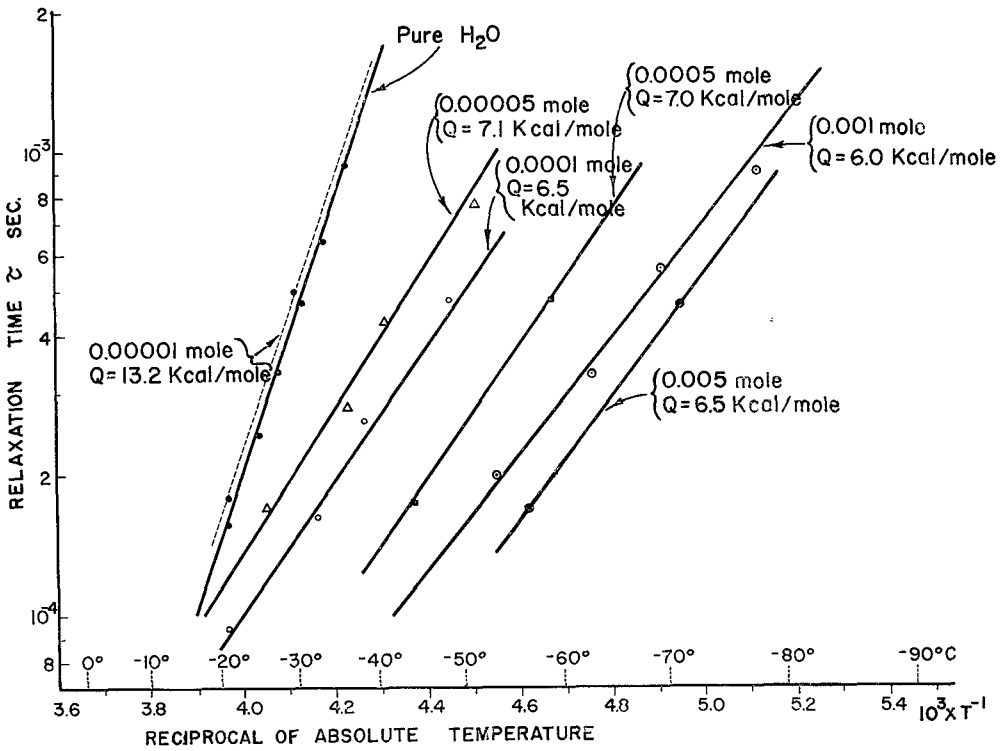

Fig. 14. Relaxation time of NaCl-doped ice as a function of concentration

shifted towards the low temperature ranges with increase in concentration. The mound-like damping at low tmperature was seen at higher concentrations. Grain boundary internal friction also increased with an increase in the NaCl concentration.

Figure 14, illustrates the logarithmic plots of relaxation time vs. T'^{-1} for various NaCl concentrations. The $\log\tau - T'^{-1}$ curve for the most dilute specimen (0.00001 mole) is located at the same temperature range as pure ice, having the activation energy $Q=13.2$ kcal/mole. The slope of the $\log\tau - T'^{-1}$ curve became less at concentrations above 0.00005 mole but maintained about the same slope. Consequently, the activation energies are all close to 6.6 kcal/mole. The location of the $\log\tau - T'^{-1}$ curve shifted toward the low temperature range as a function of the increased NaCl concentration.

4. *Modification of Mechanical Damping due to HF and NH_4F*

Fluoride ions have been regarded as one of the most favorable substances to make a solid solution with ice. TRUBY (1955) in his X-ray study concerning the lattice constant of fluoride-doped ice crystals, found that a fluorine atom can occupy substitutionaly the site of oxygen without any distortion of the ice unit cell. The diameters of the fluorine and oxygen atoms are nearly the same. Therefore, the difference in the manner in which mechanical damping is modified should depend upon whether the impurity atoms enter into the ice crystal lattice either interstitially, or substitutionally. Two HF-doped ice crystals were made by freezing of aqueous solutions containing 0.005 mole and 0.0025 mole of HF. The electrical resistivities of melted water from these specimens were 350 kohm cm and 500 kohm cm, respectively.

Figure 15 illustrates the temperature dependence of the mechanical damping of HF-doped ice obtained from 0.005 mole solution. The two solid curves represent observed data for the fundamental and first overtone vibrations. The relaxation curves become broad (mean $\Delta T'=41$°C), and result in a reduced activation energy $Q=5.6$ kcal/mole for proton diffusion. No peculiar damping, however, was observed in the low temperature range as seen in NaCl- or HCl-doped ice crystals. Since the fluorine atom can occupy the lattice site of the oxygen, the following reaction might be established in HF-doped ice crystals.

$$HF + H_2O \rightleftharpoons F^- + H_3O^+$$

The observed modifiaction of the relaxation curve, therefore, could be caused by the H_3O^+ ions produced by the addition of HF. Noticeable shift of the relaxation curve toward the high temperature range was observed accompanying the reduction of maximum height, after this specimen was kept at -3.0°C for 10 days. Two broken lines (indicated by arrows) in Fig. 15 represent

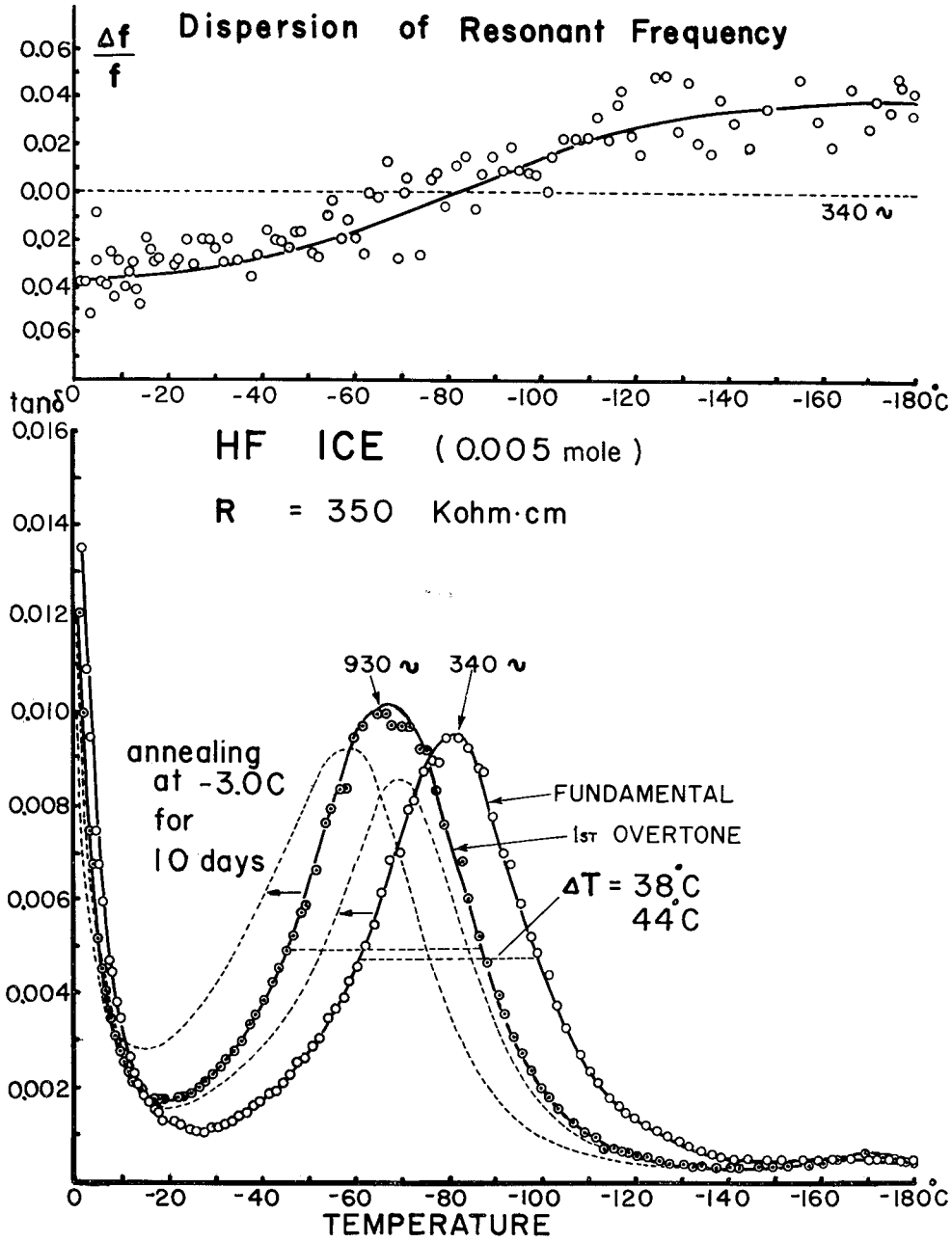

Fig. 15. Temperature dependence of internal friction in HF-doped ice

this annealing effect.

In Fig. 16, curve (a) shows the logarithmic plots of the relaxation time of this specimen against T^{-1}. After annealing at -3.0°C for 10 days, curve (a) shifted to (b). Curve (c) represents $\log \tau - T^{-1}$ for the specimen produced from the solution containing 0.0025 mole HF.

Conspicuous modification and the annealing effect on the mechanical damping curve was also observed in the NH_4F-doped ice crystals. The specimen was made from an aqueous solution containing 0.01 mole NH_4F. The

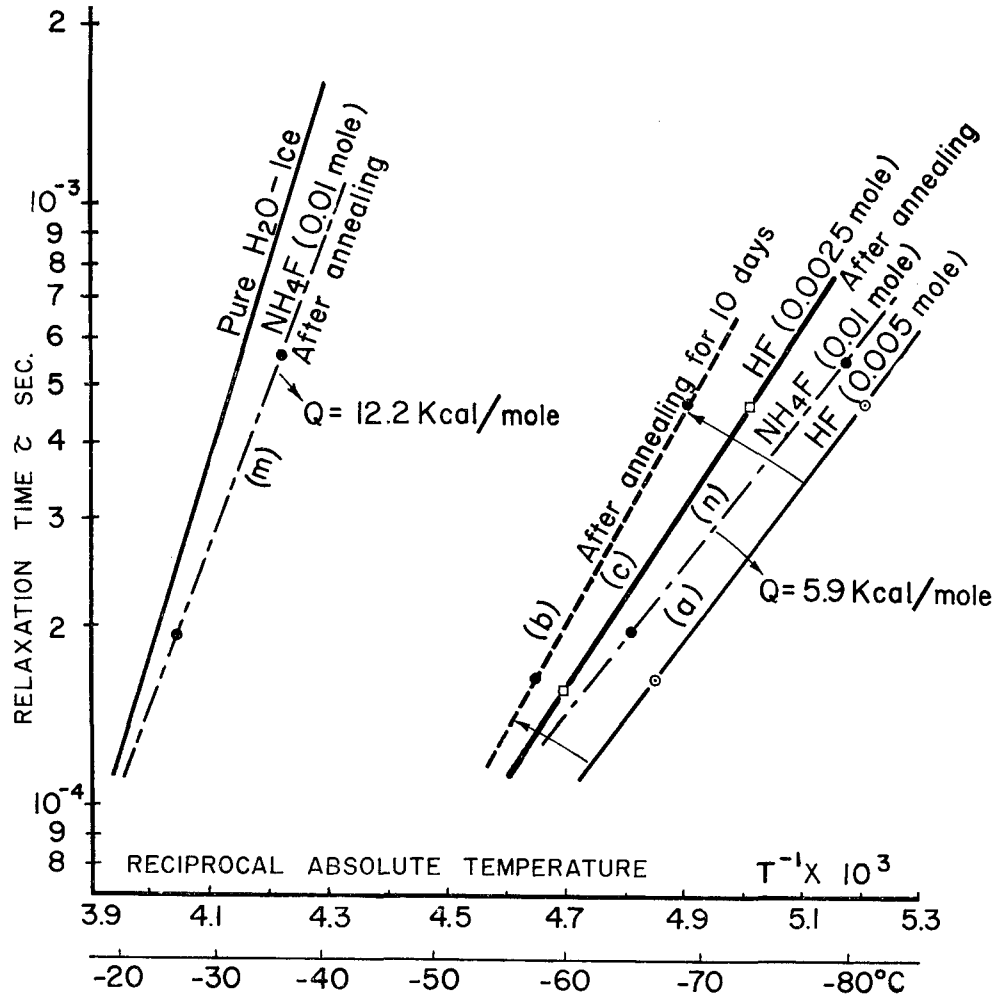

Fig. 16. Relation between relaxation time of HF- and NH_4F-ice crystals and the reciprocal of absolute temperature

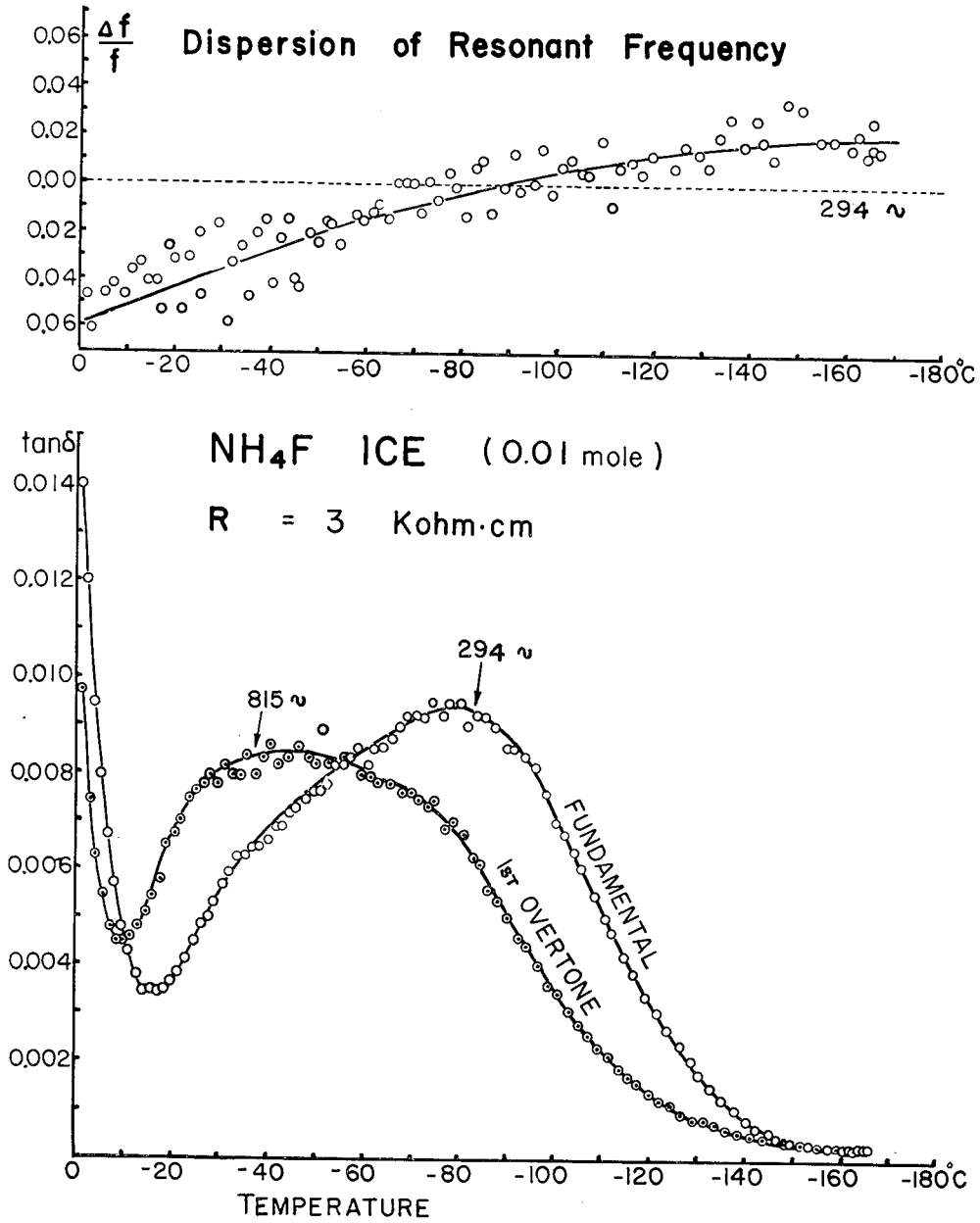

Fig. 17. Temperature dependence of internal friction in NH_4F-ice (before annealing)

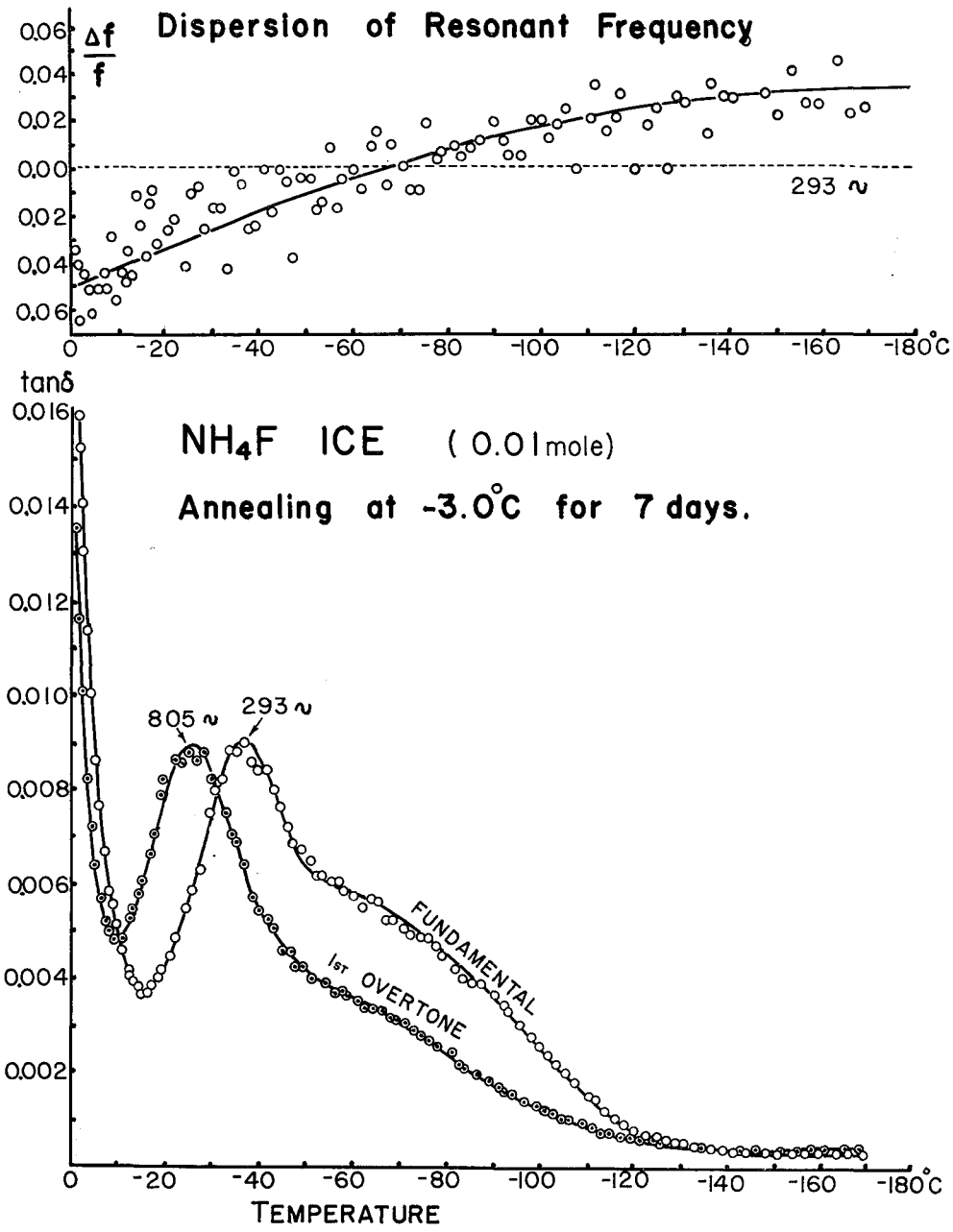

Fig. 18. Variation of tan δ after 7 days of annealing at −3.0°C

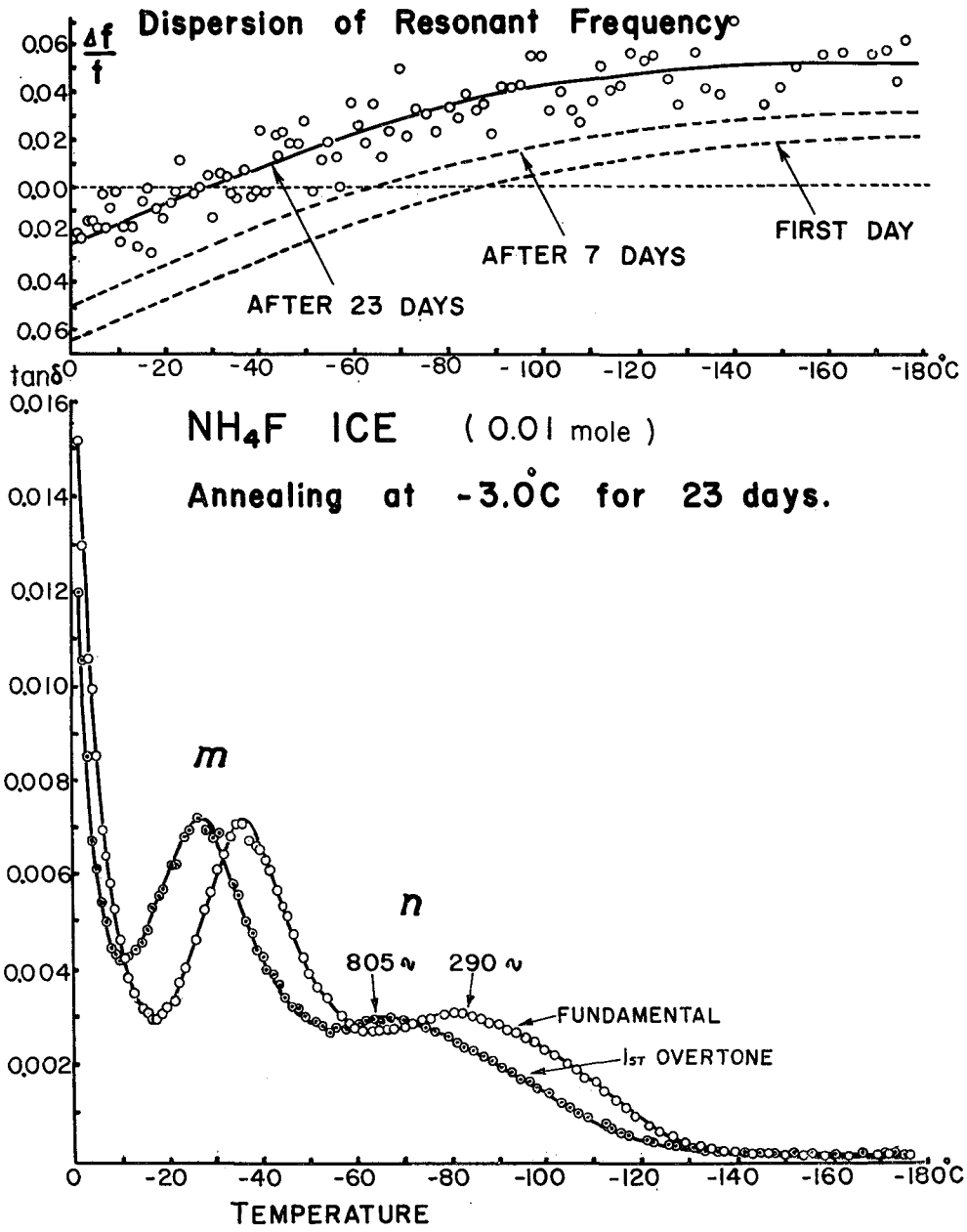

Fig. 19. Variation of tan δ after 23 days of annealing at −3.0°C. Two maxima m and n appeared on each curve

electrical resistivity of this melted specimen was only 3 kohm cm. Figure 17 illustrates mechanical damping curves measured at the fundamental, and at the first overtone vibrations. The relaxation curve became very broad ($\Delta T = 88°C$) and the location of maximum damping was difficult to determine. Dispersion of resonant frequency took place throughout the entire temperature range. After the first measurement, this specimen was put in a polyethylene envelope and annealed at $-3.0°C$. Figure 18 and Fig. 19 illustrate the variation in damping for 7 and 23 days annealing periods. After 7 days of annealing, a noticeable maximum appeared on each curve, reducing the height of damping on the low temperature side. After 23 days elapsed, two distinguishable maxima were observed on the damping curve as indicated by m and n showing that the location of both maxima shifted toward a higher temperature range with increased frequency.

The $\log \tau - T^{-1}$ curves obtained for both m and n maxima are plotted in Fig. 16. Curve m is located nearly in the same temperature range as pure ice, with a steep slope $Q = 12.2$ kcal/mole. The appearance of the separate maxima in the relaxation curves can be ascribed to the internal change in chemical composition of the specimens. It is supposed that these changes were caused gradually by annealing, which can form nearly impurity free regions within doped ice crystals. According to BRILL and CAMP (1961), NH_4F may decompose in solid solution to the following two components:

$$2NH_4F \longrightarrow NH_3 + NH_4 \cdot HF_2 .$$

NH_3 generated by this decomposition may be in a gaseous state. Since occlusion of the gaseous ammonia in ice is very difficult, it may be diffused out from the inside of grains to the crystal surfaces, leaving an NH_3 free zone. The impossibility of the occlusion of NH_3 in ice is easily demonstrated by freezing of the ammonia solution. An aqueous solution containing 0.005 mole of NH_3 was frozen, and a specimen was prepared. The internal friction was measured at both fundamental (312 c.p.s.) and the first overtone (865 c.p.s.) vibrations. Sharp relaxation curves were observed in the same temperature range as pure ice, showing that $\Delta T = 23°C$ and the activation energy $Q = 12.5$ kcal/mole. No peculiar damping was observed in the low temperature range. In fact, the electrical resistivity of this melted specimen was found to be 1200 kohm cm (approximately the same as pure ice crystals), implying that the occlusion of ammonia was difficult even at the grain boundaries. It can be concluded that long annealing of NH_4F-ice near the melting point results in the separation of nearly pure crystals from doped crystal regions as indicated by m and n in Fig. 19.

In NaCl-doped ice crystals, the minimum concentration which had no

influence on mechanical damping was 10^{-5} mole as shown in Fig. 14. In substitutional impurities, however, the modification of the relaxation curve may be observed at much lower concentrations. In order to determine the minimum concentration of NH_4F, the ice specimens were made by freezing various dilute solutions. The specimen made by freezing a 10^{-7} mole NH_4F solution, showed relaxation curves similar to those of pure ice as illustrated by broken lines in Fig. 20 ($\Delta T=24°C$). When the concentration of NH_4F was increased to $5\cdot10^{-7}$ mole, an obvious change was observed on the low temperature side of the relaxation curves, depicted by solid lines. The measured frequencies for the fundamental and the first overtone vibrations are indicated on each curve. The modification of the relaxation curve became conspicuously related to the concentration of NH_4F. At higher concentrations above 10^{-4} mole, it was difficult to determine precisely the location of maximum internal

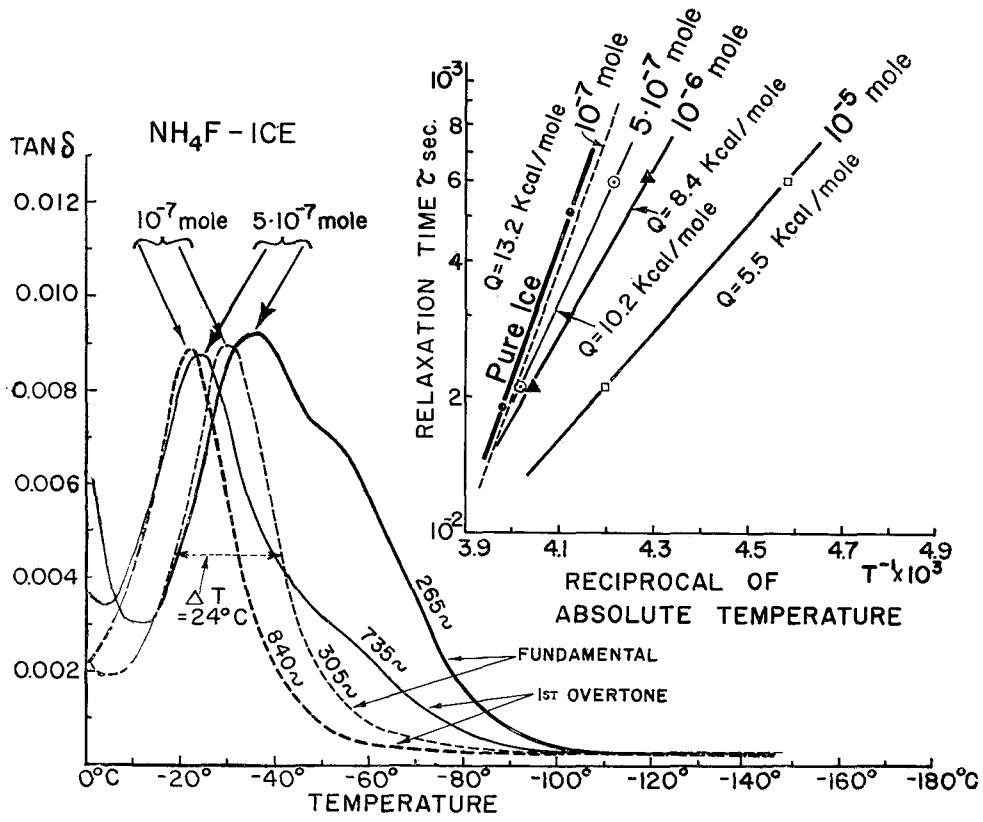

Fig. 20. Modification of the NH_4F-doped ice relaxation curves as a function of concentration

friction because of the broadness of the damping curve. As shown in Fig. 20, $\log \tau - T^{-1}$ curves shifted toward the low temperature side with increased concentration, and the accompanying decrease in slope indicates the decreased activation energy. Similar phenomena have been observed in the dielectric properties of solid solutions of ice and NH_4F by ZAROMB and BRILL (1956). The minimum concentration of NH_4F having no significant influence on mechanical damping must be between 10^{-7} mole and $5 \cdot 10^{-7}$ mole. Therefore NH_4F can modify the ice lattice structure even at extremely low concentrations.

V. Resultant Mechanical Damping Curves of Artificially Combined Ice Crystals

The curve in Fig. 19 has been explained as a resultant of two kinds of relaxation curves, shown by m and n. A more concrete model concerning this problem can be demonstrated by use of artificially combined crystals.

A laboratory-made pure single crystal bar and a contaminated natural single crystal bar were welded at the center, and trimmed with a microtome to the dimensions shown in A of Fig. 21. P is the laboratory-made pure ice, Q is a natural contaminated single ice crystal. The electrical resistivity of the melted specimen of Q was 450 kohm cm. The natural ice crystal was obtained from Lake Shikaribetsu, located in Hokkaido, Japan. As the lake ice consisted of fairly large grains (approximately 3 to 4 cm in diameter, 30 to 40 cm long), a single ice crystal bar was easily cut from one grain. Two broken lines, P and Q, show the relaxation curves which would be obtained if the 172 mm long specimen were composed of a pure or of a contaminated single ice crystal only. The damping maxima of the pure and contaminated ice are located at $-32°C$ and $-63°C$, respectively. The height of maximum damping of Lake Shikaribetsu's ice was remarkably lower than that of the artificially made crystal because of the orientation of its c-axis (see next section). In Fig. 21 A, a thick and a thin solid curves represent the resultant mechancal damping of this combined crystal measured at the fundamental (320 c.p.s.) and the first overtone (890 c.p.s.) vibrations, respectively.

Another specimen was prepared in which the pure and the contaminated ice crystals were welded with a broad contact area, and then trimmed to the dimensions illustrated in Fig. 21 B. The resultant mechanical damping obtained at the fundamental and the first overtone vibrations are shown by thick and thin solid curves.

These curves are quite similar to the final stage of annealing in the NH_4F-doped specimen as seen in Fig. 19. The contaminated and the pure crystals exhibit their individual dampings in the lower and higher temperature ranges,

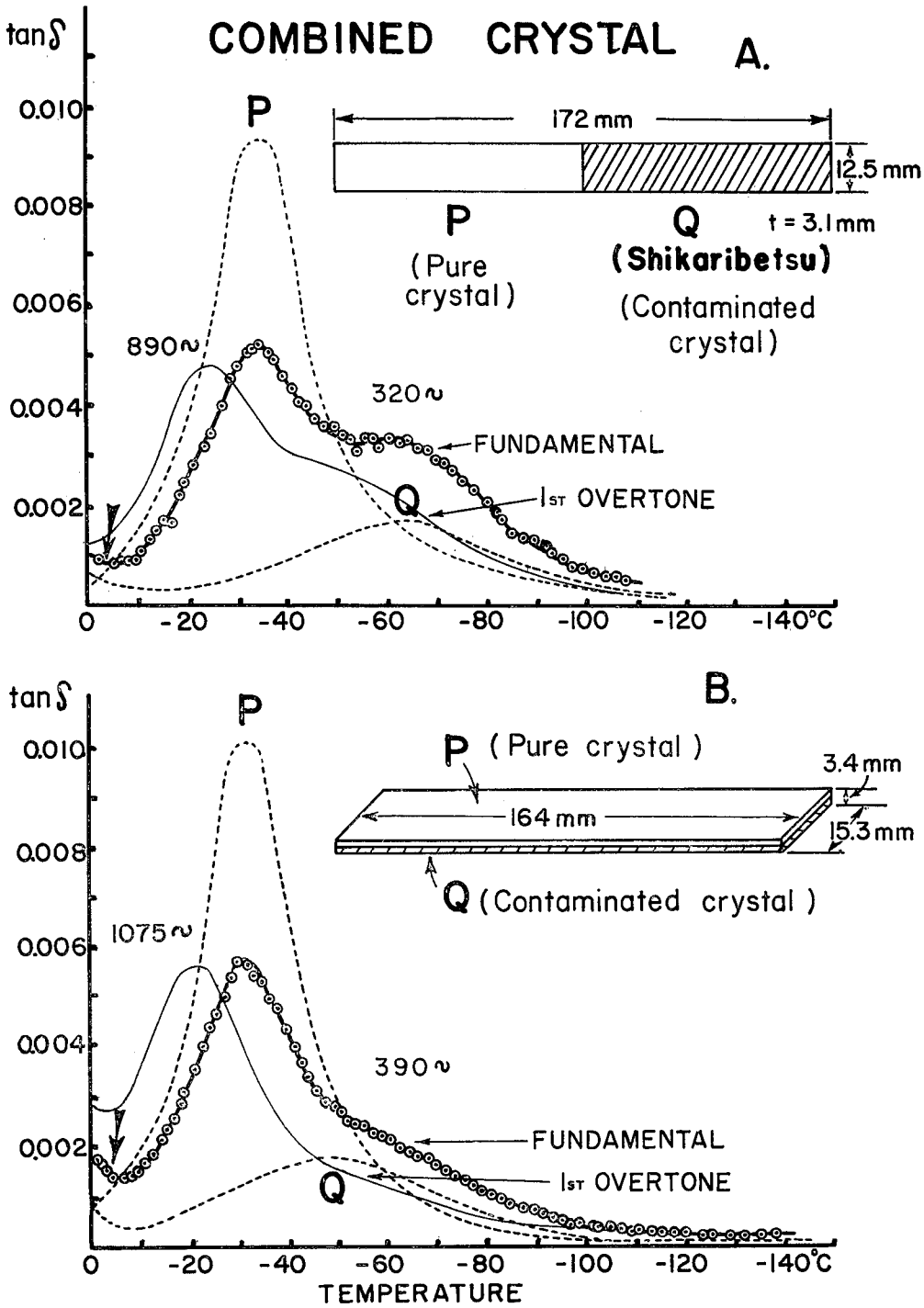

Fig. 21. Resultant damping curves for artificially combined crystals

respectively.

VI. Anisotropy of the Height of Maximum Damping Due to Crystallographic Orientation; and the Influence of Plastic Deformation on Maximum Damping

In our experiment, the height of maximum damping due to proton movement in randomly oriented polycrystalline ice was between 0.0105~0.008 (mean 0.009) in the frequency ranges of 170 c.p.s. to 2200 c.p.s. Most specimens of pure or dirty ice showed a slight decrease in the height of maximum damping with increasing frequency. P. SCHILLER (1958) found that the height of maximum damping of specimens having their c-axis parallel to the direction of the longitudinal oscillation was 1/6 of that of the specimens having their c-axis perpendicular to the direction of the oscillation. A similar relationship between maximum damping and crystallographic orientation was also revealed in our experiments by the flexural vibration.

Three different specimens of single crystal ice having different orientations were prepared as depicted in Fig. 22 (A), (B) and (C). Specimens (A) and (B) were cut from the same slightly contaminated ice crystal made in the laboratory. Specimen (C) was prepared from a natural single crystal of ice obtained from Lake Shikaribetsu. When the specimens (A) and (B) were set in the flexural vibration, the basal planes of (A) and the c-axis of (B) were perpendicular to each neutral plane. In the specimen (C), the c-axis was parallel to the neutral axis through the bar. In Fig. 22, curves (a) (white squares and solid line) and (b) (white circle and broken line) show the mechanical damping of specimens (A) and (B) obtained at the fundamental frequency. No difference was observed in the height of either maximum, but appreciable difference was found in their damping at low temperatures due to chemical impurities as indicated by an arrow in Fig. 22. In the middle part of Fig. 22, this difference is illustrated with an ordinate enlargement of five. Curve (c) represents the maximum damping of specimen (C) showing 1/5 of the value of (A) or (B). When a specimen was prepared from the same Lake Shikaribetsu's ice so that the direction of the c-axis was perpendicular to the neutral plane as shown in (B), the height of its maximum damping coincided with (B).

In order to examine how the height of its maximum damping could be modified by plastic deformation, specimen (C) was bent at $-25°C$ by supporting it at both ends and loading it at the center. After 2 days, depression of the center of the ice bar due to loading was about 15 mm. Then the specimen was turned over and reloaded at the center until the ice bar was straightened. The mechanical damping was measured again, but no change of the height of

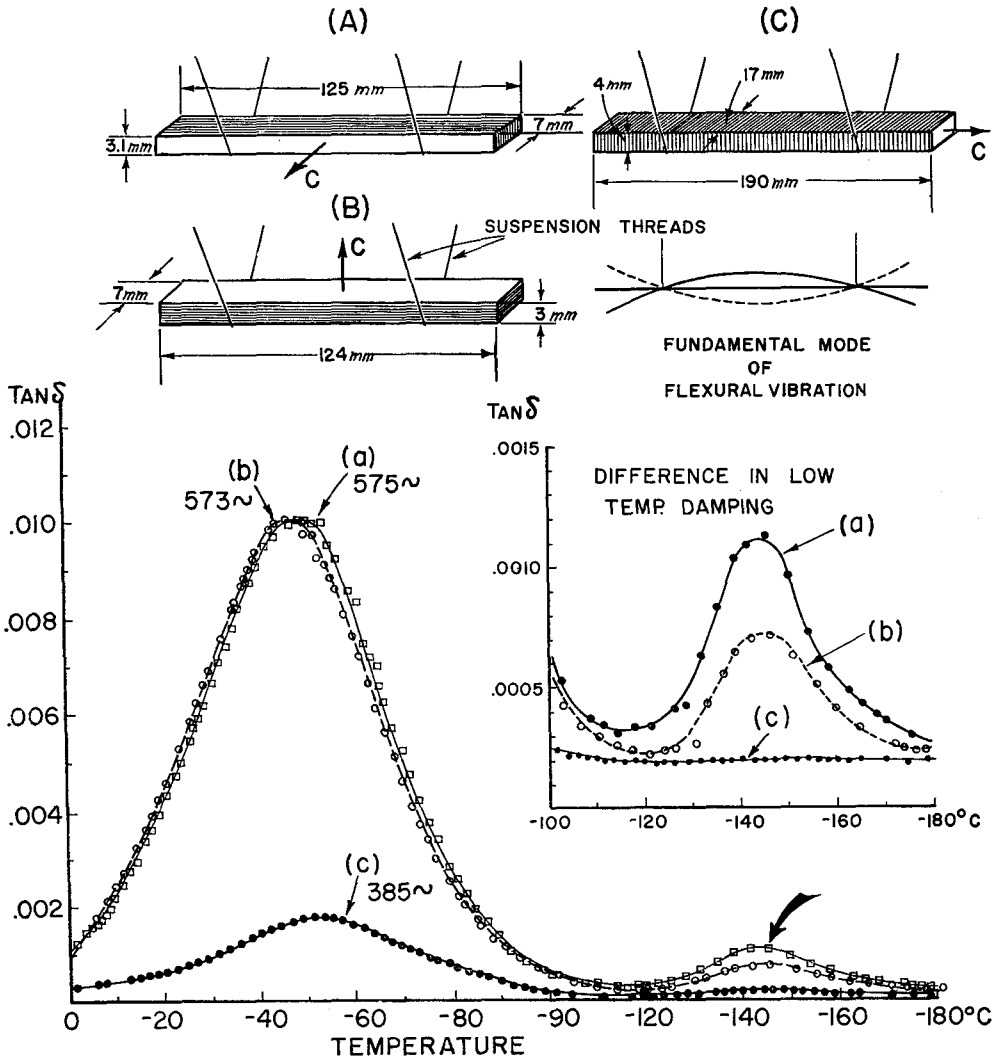

Fig. 22. Anisotropy of internal friction due to c-axis orientation

maximum damping was observed, implying that these deformations did not have any influence on the proton movement. Another specimen was prepared from a previously deformed single crystal and compared with a non-deformed specimen. In this case, no difference again was observed between the two damping maxima, suggesting that plastic deformation can not change the total number of lattice defects.

VII. Concluding Remarks

The internal friction of ice was measured by the flexural vibration method, between 0°C and −180°C, thus the influence of chemical impurities was revealed. Mechanical relaxation curves observed in pure H_2O and D_2O ice, were narrow and sharp, and they appeared in high temperature ranges. Activation energy Q, and the preexponential factor agreed with those obtained by the dielectric relaxation method, implying that anelasticity in ice crystals is attributable to proton movement through lattice defects.

Contaminated ice crystals were made with various kinds of chemical additives. In doped ice crystals, the relaxation curves became broad and maximum damping appeared in temperature ranges lower than that of pure ice. The observed relaxation time also shortened and the activation energy became half the pure ice value, implying that many lattice defects which contribute to proton movement are produced by chemical impurities. In NaCl-doped ice crystals, appreciable effect was observed in specimens made from solutions having concentrations above $5 \cdot 10^{-5}$ mole. In NH_4F-doped ice crystals, however, the lowest concentration that had an effect on mechanical damping was between 10^{-7} mole and $5 \cdot 10^{-7}$ mole.

Anisotropy of the height of maximum damping was investigated by use of single ice crystals having different crystallographic orientations. The height of maximum damping of the specimens having c-axis parallel to the neutral line of the flexure vibration decreased to about 1/5 of that of the specimen in which the c-axis was perpendicular to the neutral line.

Another kind of damping caused by chemical impurities concentrated in aggregates was observed in the low temperature range (around −145°C). The behavior of this damping is quite different from the anelasticity due to proton movement. The height of damping in this case was reduced with increase of frequency and also by heat treatment. This damping probably was caused by oscillation of impurities occluded at localized imperfections such as microscopic holes or vacant places in the ice crystals lattice.

Acknowledgments

This work was carried out at USA CRREL, Hanover, N. H. and the Institute of Low Temperature Science, Hokkaido University, Sapporo, Japan. The author is grateful to the Directors of both research institutes, and should like to thank Mr. J. BENDER, Drs. P. CAMP, W. WEEKS, Mr. J. SAYWARD, and Dr. J. WEERTMAN (Northwestern Univ.) for useful discussions and PEC. P. SELLMANN U.S. Army for help in preparing this paper. The author also

wishes to express his sincere thanks to Mr. SHINDO (Fukuoka Sangyo Co.) for making the experimental apparatus.

References

AUTY, R. P. and COLE, H. 1952 Dielectric properties of ice and solid D_2O. J. Chem. Phys., **20**, 1309–1314.

BJERRUM, N. 1952 Structure and properties of ice. Science, **115**, 385–390.

BRILL, R. and CAMP, P. 1961 Properties of ice. USA CRREL Research paper, No. 68.

GRANICHER, H., JACCARD, C., SCHERRER, P. and STEINEMANN, A. 1957 Dielectric relaxation and the electrical conductivity of ice crystals. Disc. Fara. Soc., **23**, 50–62.

KINGERY, W. D. 1960 Regelation, surface diffusion and ice sintering. J. App. Phys., **31**, 833–838.

KNESER, H. O. et al. 1955 Mechanische Relaxation von Einkristallinem Eis. Naturwiss., **15**, 437.

KUROIWA, D. and YAMAJI, K. 1956 Visco-elastic property of ice in the temperature range 0°～−100°C. I. Low Temperature Science, **A 15**, 171–184.

KUROIWA, D. and YAMAJI, K. 1959 Internal friction of Poly- and single-crystal ice. Low Temperature Science, **A 18**, 97–114.

KUROIWA, D. 1961 A study of ice sintering. Tellus, **2**, 252–259.

NAKAYA, U. 1956 Properties of single crystals of ice, revealed by internal melting. USA SIPRE Research Paper, **13**, 80. pp.

SCHILLER, P. 1958 Die Mechanische Relaxation in Reinen Eiseinkristallen. Z. Physik, **153**, 1–15.

SMYTH, C. P. and HITCHCOCK, C. S. 1932 Dipole rotation in crystalline solids. J. Amer. Chem. Soc., **54**, 4631–4647.

TRUBY, F. K. 1952 A study of the electrical properties of ice. Contract Nonr-815(01), Project Designation No. NR-082-092.

TRUBY, F. K. 1955 Latice constants of pure and fluoride contaminated ice. Science, **121**, 404.

ZAROM, S. and BRILL, R. 1956 Solid solution of ice and NH_4F and their dielectric properties. J. Chem. Phys., **24**, 895–902.